A single-substrate model to interpret intra-annual stable isotope signals in tree-ring cellulose

J. OGÉE[1], M. M. BARBOUR[2], L. WINGATE[1,3], D. BERT[1], A. BOSC[1], M. STIEVENARD[4], C. LAMBROT[1], M. PIERRE[4], T. BARIAC[5], D. LOUSTAU[1] & R. C. DEWAR[1]

[1]*Ephyse, Inra, Bordeaux, BP81, 33883 Villenave d'Ornon, France,* [2]*Landcare Research, PO Box 40, Lincoln 7640, New Zealand,* [3]*School of GeoSciences, IAES, University of Edinburgh, Edinburgh EH9 3J, UK,* [4]*LSCE, CEA/Cnrs, 91191 Gif/Yvette, France and* [5]*BIOEMCO, Cnrs/Inra/UPMC, 78850 Thiverval-Grignon, France*

ABSTRACT

The carbon and oxygen stable isotope composition of wood cellulose ($\delta^{13}C_{cellulose}$ and $\delta^{18}O_{cellulose}$, respectively) reveal well-defined seasonal variations that contain valuable records of past climate, leaf gas exchange and carbon allocation dynamics within the trees. Here, we present a single-substrate model for wood growth to interpret seasonal isotopic signals collected in an even-aged maritime pine plantation growing in South-west France, where climate, soil and flux variables were also monitored. Observed seasonal patterns in $\delta^{13}C_{cellulose}$ and $\delta^{18}O_{cellulose}$ were different between years and individuals, and mostly captured by the model, suggesting that the single-substrate hypothesis is a good approximation for tree ring studies on *Pinus pinaster*, at least for the environmental conditions covered by this study. A sensitivity analysis revealed that the model was mostly affected by five isotopic discrimination factors and two leaf gas-exchange parameters. Modelled early wood signals were also very sensitive to the date when cell wall thickening begins (t_{wt}). Our model could therefore be used to reconstruct t_{wt} time series and improve our understanding of how climate influences this key parameter of xylogenesis.

Key-words: carbon cycle; carbon isotope; dendroclimatology; oxygen isotope; water cycle; xylogenesis.

INTRODUCTION

More than 30 years ago, several authors proposed that the oxygen isotope composition of wood may be viewed as an 'isotopic thermometer' (Schiegl 1974; Gray & Thompson 1976; Libby *et al.* 1976; Wilson & Grinsted 1977). Following this lead, a large number of studies attempted to reconstruct past climates by applying simple empirical functions relating the carbon or oxygen isotope composition of whole wood (or cellulose extracted from wood) to temperature, relative humidity, soil moisture or rainfall [see Switsur & Waterhouse (1998) and references therein]. However, the degree of correlation between observed isotope ratios and

environmental parameters is quite variable among studies. A recent review (McCarroll & Loader 2004) concluded that the search for a single or even dual set of environmental drivers that control the stable isotope composition of wood is 'futile'. Instead a comprehensive approach that embraces existing mechanistic understanding of all the processes involved is required.

More recently, these signals have also been proposed as good recorders of plant water use efficiency and stomatal or photosynthetic regulation (Saurer, Aellen & Siegwolf 1997; Scheidegger *et al.* 2000; Barbour, Walcroft & Farquhar 2002). This is because, at the leaf level, the stable carbon isotope composition of recently assimilated carbohydrates ($\delta^{13}C_{assimilates}$) is known to reflect the leaf intrinsic water-use efficiency, defined as the ratio of leaf photosynthesis and stomatal conductance (Farquhar & Richards 1984), whereas the oxygen isotope composition of the same photoassimilates ($\delta^{18}O_{assimilates}$) is more a recorder of leaf evaporative demand (Saurer *et al.* 1997; Barbour & Farquhar 2000).

Most studies assume that wood is formed from recently assimilated carbohydrates, so that the isotopic fractionation during leaf gas exchange, which is strongly related to drought and climate, is 'frozen' in wood cellulose. This assumption has been critically examined by several authors (Walcroft *et al.* 1997; Klein *et al.* 2005; Skomarkova *et al.* 2006), who combined high-resolution tree-ring carbon isotopic data and a process-based model of photosynthetic discrimination against $^{13}CO_2$ to examine the degree to which the photosynthetic signal was recorded in annual rings of trees. These studies find some degree of correlation between the two seasonal cycles, but clearly show smaller synoptic amplitude in the biomass signal, supporting the idea that post-photosynthetic processes, such as the mixing of sugars during phloem transport, must be accounted for. The idea that recently assimilated sugars enter and mix in a larger pool before being incorporated into the wood is also supported by several studies on the dynamics of isotopic signals in phloem sugars (Gessler, Rennenberg & Keitel 2004; Barbour *et al.* 2005; Brandes *et al.* 2006).

In fact, several post-photosynthetic processes may compromise a simple transfer of leaf-level isotopic signals to annual tree rings (Hemming *et al.* 2001; Helle & Schleser

Correspondence: J. Ogée. Fax: +33 557 122430; e-mail: jogee@ bordeaux.inra.fr

2004; Schultze *et al.* 2004; Skomarkova *et al.* 2006). Hemming *et al.* (2001) advanced a detailed process model of carbon allocation and cambial activity to study the influence of some post-photosynthetic processes on $\delta^{13}C_{cellulose}$ and concluded that storage of carbohydrates and their re-mobilization can potentially have a greater influence on $\delta^{13}C_{cellulose}$ than seasonal variations in environmental conditions. Helle & Schleser (2004) illustrated this caveat with multiple examples of high-resolution intra-annual measurements of carbon isotope variations recorded in the cellulose of several deciduous trees. These time-series exhibited a sharp enrichment in the $^{13}C/^{12}C$ ratio of wood formed during early spring, a period when discrimination during photosynthesis was expected to lead to relatively depleted values. Re-mobilization of an enriched pool of storage starch and discrimination during respiration were proposed as possible mechanisms to explain this ^{13}C enrichment at the beginning of the early wood. A recent pulse-labelling study on naturally growing *Larix gmelinii* saplings demonstrated that the re-mobilization of stored starch from 1 year to the next is not restricted to broad-leaved species, but can occur on evergreen species as well, especially in cold climates (Kagawa, Sugimoto & Maximov 2006).

The model of Hemming *et al.* (2001) is probably the most advanced model to interpret carbon isotope signals in tree rings and is biologically instructive in its attempt to represent the complexity of a natural phenomenon. However, the number of parameters required to run this model is too large (69 parameters for the cambial activity model alone and more than 150 parameters for the full model), making it impractical to routinely parameterize for different species growing in the field. It is also restricted to carbon isotope signals only. For oxygen isotope signals in wood cellulose, the most comprehensive model (Roden, Lin & Ehleringer 2000; Barbour *et al.* 2002), does not include post-photosynthetic processes, apart from the exchange of oxygen atoms with 'sink' water during cellulose synthesis. More importantly, some theoretical aspects of this model remain untested, especially under field conditions (Cernusak, Farquhar & Pate 2005). Furthermore, and quite surprisingly, direct and quantitative comparisons of modelled and measured isotope ratios in wood cellulose are rare and restricted to $\delta^{13}C$ signals only (Walcroft *et al.* 1997; Hemming *et al.* 2001; Klein *et al.* 2005; Skomarkova *et al.* 2006) or $\delta^{18}O$ signals only (Roden *et al.* 2000).

In this paper, we present a model of both carbon and oxygen isotope signals in tree-ring cellulose that accounts for two important post-photosynthetic factors: (1) the mixing of recent assimilates during phloem transport; and (2) the time taken for cellulose deposition in new bark and xylem cells during wood formation. The model is much simpler than in Hemming *et al.* (2001) and is extended to oxygen isotopes. We wished to test the simplifying hypothesis that starch storage and re-mobilization could be neglected and therefore did not include these processes in our model. This 'single-substrate' hypothesis and the new model are then tested against a high-resolution intra-annual $\delta^{13}C$ and $\delta^{18}O$ cellulose record

contained in two annual rings of maritime pine trees (*Pinus pinaster* Ait.) growing in a even-aged, multi-instrumented flux site in south-western France. This site was notably equipped with sap flow and dendrometer sensors, therefore reducing the number of 'unknown' model parameters and their uncertainties. A sensitivity analysis of the model to the most uncertain parameters is also presented.

MODEL DESCRIPTION AND MAIN ASSUMPTIONS

Total carbon budget of the water-soluble sugar pool

In the allocation model described by Hemming *et al.* (2001) three biomass compartments are distinguished: leaves (new and old); stem wood (including coarse roots); and fine roots. In addition, these biomass compartments have specific, individualized pools of starch and share a common pool of water-soluble sugars. Furthermore, respiration and wood synthesis are assumed to use water-soluble sugars as a first priority, so that re-mobilization from each starch pool is important only when the water-soluble sugar pool becomes limiting (at time scales relevant for wood synthesis, that is weeks, leaf transitory starch can be included in the water soluble sugar pool). In this study, we assume that non-structural carbon in the tree is represented by a single and well-mixed pool of water-soluble sugars, which is assumed to be always large enough to supply the metabolic demand during the growing season (Fig. 1a). This pool of sugars comprises leaf, wood and fine root sugars and is filled by leaf net photosynthesis (including leaf photorespiration and mitochondrial respiration) F_{leaf} (expressed at the stand level in kgC m^{-2} ground area s^{-1}) and used as substrate for maintenance and growth woody respiration F_{wood} (kgC m^{-2} ground area s^{-1}) and whole-tree biomass synthesis $S_{biomass}$ (kgC m^{-2} ground area s^{-1}). The carbon budget of the pool can then be written as

$$\frac{dC_{pool}}{dt} = F_{leaf} - F_{wood} - S_{biomass}, \tag{1}$$

where C_{pool} (kgC m^{-2} ground area) is the size of the sugar pool. Biomass production is assumed to be carbon-limited. In line with our objective to keep the model as simple as possible, and following previous substrate-based models of plant growth [e.g. Dewar, Medlyn & McMurtrie (1998)], we assume a linear relationship between $S_{biomass}$ and C_{pool}, that is,

$$S_{biomass} = k_{pool}C_{pool}, \tag{2}$$

in which k_{pool} (s^{-1}) is a constant rate coefficient. Equation 1 can then be re-written as

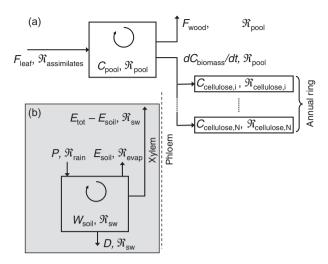$$\frac{dC_{pool}}{dt} + k_{pool}C_{pool} = F_{leaf} - F_{wood}. \tag{3}$$

Figure 1. (a) The single-substrate tree pool model. The well-mixed pool is fed by photosynthesis (F_{leaf}) with isotopic signature $\Re_{assimilates}$ and used as the substrate for wood respiration (F_{wood}) and biomass synthesis ($dC_{biomass}/dt$), with an isotopic signature $\Re_{pool}$. A proportion of the new biomass is allocated to each ring section ($i = 1, N$), with a final cellulose content $C_{cellulose,i}$ and isotope ratio $\Re_{cellulose,i}$. (b) The soil water pool model. The well-mixed pool is fed by precipitation (P) with isotopic signature $\Re_{rain}$ and used for soil evaporation (E_{soil}), with an isotopic signature $\Re_{evap}$, canopy and understorey transpiration ($E_{tot} - E_{soil}$) or deep drainage (D), with an isotopic signature $\Re_{sw}$.

Equation 2 suggests (very crudely) that biomass production is a passive process, solely governed by the amount of carbohydrates in the tree. In this framework, the model parameter k_{pool} can be seen as the pool turnover rate. Although plant growth is undoubtedly more complex than this, our aim was to first evaluate to what extent this simple model was able to capture seasonal patterns in isotope composition, before adding more complexity.

Carbon and oxygen isotope signals of the sugar pool

The budget equation of ^{13}C or ^{18}O atoms in the sugar pool can be written in a similar fashion as for total carbon (Eqn 1). We denote by $\Re_{pool}$ the average (carbon or oxygen) isotope ratio of sugars in the well-mixed pool. At natural abundance stable isotope ratios are small compared with unity ($\Re << 1$) so that the 'light' sugar is the most abundant in the pool and its amount is close to C_{pool}. The budget equation of ^{13}C or ^{18}O atoms in the sugar pool is then

$$\frac{d(C_{pool}\Re_{pool})}{dt} = F_{leaf}\Re_{assimilates} - F_{wood}(1-e)\Re_{pool} - \qquad (4)$$
$$k_{pool}C_{pool}(1-x)\Re_{pool},$$

where $\Re_{assimilates}$ is the isotope ratio of current assimilates entering the pool and e and x are isotope fractionations associated with wood respiration and biomass synthesis, respectively. Subtracting Eqn 3 (multiplied by $\Re_{pool}$) from Eqn 4 leads to

$$\frac{d\Re_{pool}}{dt} - xk_{pool}\Re_{pool} = \frac{1}{C_{pool}} \cdot [F_{leaf}(\Re_{assimilates} - \Re_{pool}) + \qquad (5)$$
$$eF_{wood}\Re_{pool}].$$

In other words the rate of change of the isotope ratio in the sugar pool is driven by the difference $\Re_{pool} - \Re_{assimilates}$, and the isotope fractionations e and x. The recorded signal in $\Re_{pool}$ is therefore attenuated and delayed compared with the signal in $\Re_{assimilates}$.

The isotope ratio of current assimilates is related to leaf gas-exchange signals driven by climate variables such as light, air vapour pressure deficit (VPD) and soil conditions. For both ^{13}C and ^{18}O isotopes, well-established theoretical models exist allowing us to relate $\Re_{assimilates}$ to leaf photosynthesis or stomatal conductance. These models are summarized in Appendix A.

In the framework of our single-substrate model, we will not try quantifying the contribution to the overall respiratory flux of all CO_2-emitting pathways with their discrimination factors and uncertainties (except photorespiration, see Appendix A). Instead, we will test the simplifying situation where only one single discrimination factor e, as seen from this single substrate pool and expressed relatively to its isotope composition $\Re_{pool}$, is accounted for.

Cernusak *et al.* (2005) observed that the ^{13}C/^{12}C ratio of cellulose extracted from recently differentiated xylem tissues matched that of simultaneously collected phloem sap sugars, suggesting no carbon isotopic fractionation during wood cellulose synthesis. In contrast, the ^{18}O/^{16}O ratio of cellulose is known to reflect only partially that of phloem sap sugars, because, during cellulose synthesis, some oxygen atoms re-exchange with water in the developing cell (Sternberg, Niro & Savidge 1986; Farquhar, Barbour & Henry 1998). However, this isotopic effect should not affect the substrate pool, but only the isotope composition of the cellulose (see the following discussion on carbon and oxygen isotope signal in wood cellulose). But wood is made of other constituents than cellulose and differences in the isotope composition of cellulose and wood dry matter for mature xylem tissues are commonly observed, for both carbon (Wilson & Grinsted 1977; Loader, Robertson & McCarroll 2003; Schultze *et al.* 2004) and oxygen isotopes (Gray & Thompson 1977; Barbour, Andrews & Farquhar 2001). These differences are attributed in part to the lignification of xylem cells, as lignin – the other main wood component – has very different biochemical pathways compared with cellulose (Whetten & Sederoff 1997). As a consequence, lignin is usually depleted compared with cellulose by 2 to 4‰ for ^{13}C atoms (Wilson & Grinsted 1977; Loader *et al.* 2003) and by up to 10‰ for ^{18}O atoms (Gray & Thompson 1977; Barbour *et al.* 2001). Isotopic effects during wood lignification but also biomass synthesis of foliage or fine roots (also accounted for in the $S_{biomass}$ term), could affect the isotope composition of the sugar pool. Lignification is not a continuous process, but occurs mainly at the end of the growing season, during xylem maturation. Foliage and fine root production also have specific

phenological phases. Accounting for isotope effects during synthesis of all these biomass compartments would imply constructing seasonal changes of the fractionation factor x, which lies beyond the scope of our study. Instead – and because we could not immediately ignore a possible isotopic effect of biomass synthesis on the isotope composition of the single-substrate pool – we assumed that the fractionation factor x was constant, in line with the way we modelled other processes like woody respiration. In this framework, it is not clear though whether x should be negative or positive. Lignin is depleted compared with cellulose but not necessarily compared with the substrate pool. In fact, because lignin is synthesized at the end of the growing season, it might be that the pool itself becomes progressively more depleted throughout the season, without implying any fractionation x.

In our model is the assumption that water-soluble sugars in the leaves, the phloem and the roots have the same isotope composition (equal to $\Re_{pool}$). This complete and instantaneous mixing of photoassimilates is clearly an approximation of reality. Indeed several studies have reported differences between ^{13}C content of leaf carbohydrates and phloem sap (Pate & Arthur 1998; Damesin & Lelarge 2003; Gessler *et al.* 2004; Scartazza *et al.* 2005) or isotopic gradients along the phloem of mature trees (Gessler *et al.* 2004; Brandes *et al.* 2006). These differences can also be caused by other processes than incomplete mixing, such as discrimination during woody respiration (e) and biomass synthesis (x) along the phloem or re-mobilization of starch reserves (Gessler *et al.* 2004) However, accounting for these processes would significantly complicate our model and is out of the scope of this study.

Carbon and oxygen isotope signal in wood cellulose

Wood formation is a succession of several steps, including cell division, cell enlargement, cell wall thickening (synthesis and deposition of cellulose, hemicellulose, proteins and lignin), cell death and finally hardwood formation [see Plomion, Leprovost & Stokes (2001) and references therein]. For each tree-ring sub-section ($i = 1, N$, where N is the number of sub-sections), we denote by $t_{0,i}$ the date at which cellulose synthesis has started and Δt_i the duration of cellulose synthesis and deposition. The amount of carbon contained in the cellulose of this tree-ring sub-section $C_{cellulose,i}$ (kgC m^{-2} ground area) is given by

$$C_{cellulose,i} = \int_{t_{0,i}}^{t_{0,i}+\Delta t_i} f_i S_{biomass} \cdot dt, \quad (6)$$

where f_i represents the fraction of the biomass increase that is allocated to the cellulose of this particular tree-ring sub-section.

Similarly, and assuming no discrimination during cellulose synthesis (Cernusak *et al.* 2005), the amount of ^{13}C atoms contained in the cellulose of this tree-ring subsection is given by

$$C_{cellulose,i} \Re_{cellulose,i} = \int_{t_{0,i}}^{t_{0,i}+\Delta t_i} \Re_{pool} \, f_i S_{biomass} \cdot dt \quad (^{13}C/^{12}C \text{ only}), \quad (7)$$

where $\Re_{cellulose,i}$ is the (carbon) isotope ratio of the tree-ring subsection. We further assume that, during the time Δt_i, the fraction f_i remains constant. Then, using Eqn 2, the carbon isotope ratio $\Re_{cellulose,i}$ is computed as

$$\Re_{cellulose,i} = \frac{\int_{t_{0,i}}^{t_{0,i}+\Delta t_i} \Re_{pool} C_{pool} dt}{\int_{t_{0,i}}^{t_{0,i}+\Delta t_i} C_{pool} dt} \quad (^{13}C/^{12}C \text{ only}), \quad (8)$$

which is independent of the allocation fraction f_i. This equation is only valid for the carbon isotope composition of wood cellulose.

As mentioned earlier, the oxygen isotope signal is complicated by the fact that, when sucrose is broken down to form cellulose, a proportion of oxygen atoms go through exchangeable carbonyl groups with surrounding water (Sternberg *et al.* 1986; Farquhar *et al.* 1998). This is characterized by a proportion p_{ex} of oxygen atoms in cellulose that have exchanged with source water during synthesis from sucrose, which is assumed to be constant in time (Barbour *et al.* 2004; Cernusak *et al.* 2005). We further assume that water in the developing cell has the same isotope composition as soil water ($\Re_{sw}$), as observed by Yakir (1998) and Cernusak *et al.* (2005). The isotope ratio of organic matter in equilibrium with source water is then given by $\alpha_{wc} \Re_{sw}$, where $\alpha_{wc} = 1 + \varepsilon_{wc}$ represents the equilibration fractionation factor between carbonyl oxygen and medium water and is expected to have a value of 1.027 (Sternberg *et al.* 1986), with some uncertainties because of the intramolecular distribution of ^{18}O atoms in the carbohydrate molecule or the incomplete equilibrium of the carbonyl hydration reactions (Sternberg *et al.* 2006). Then for ^{18}O atoms Eqn 7 must be re-written as

$$C_{cellulose,i} \Re_{cellulose,i} = \int_{t_{0,i}}^{t_{0,i}+\Delta t_i} [p_{ex} \alpha_{wc} \Re_{sw} + \quad (9)$$
$$(1 - p_{ex}) \Re_{pool}] f_i S_{biomass} \cdot dt,$$

and the oxygen isotope ratio of this tree-ring sub-section is then computed as

$$\Re_{cellulose,i} = p_{ex} \frac{\int_{t_{0,i}}^{t_{0,i}+\Delta t_i} \alpha_{wc} \Re_{sw} C_{pool} dt}{\int_{t_{0,i}}^{t_{0,i}+\Delta t_i} C_{pool} dt} + \quad (10)$$
$$(1 - p_{ex}) \frac{\int_{t_{0,i}}^{t_{0,i}+\Delta t_i} \Re_{pool} C_{pool} dt}{\int_{t_{0,i}}^{t_{0,i}+\Delta t_i} C_{pool} dt}.$$

Note that $\Re_{cellulose,i}$ depends not only on $\Re_{pool}(t)$ but also on $\Re_{sw}(t)$ at times t of the cellulose synthesis. The time evolution of $\Re_{sw}(t)$ is computed with the same degree of complexity as for $\Re_{pool}$, that is, using a simple bulk soil water budget (Fig. 1b). This is described in Appendix B.

Mechanistic models (e.g. Fritts, Shashkin & Downes 1999) describing how climate controls the rates and duration of cambial cellular processes (swelling, division, expansion and maturation) could be used to estimate the starting dates $t_{0,i}$ and duration Δt_i. This was the approach of Hemming *et al.* (2001). However, our main objective here was to test the single-substrate hypothesis and so we treated other aspects of the model empirically.

The starting dates $t_{0,i}$ indicating the creation of a new tree-ring sub-section are derived from dendrometry measurements. For that, we first assume that new bark and phloem development occurs at the beginning of the growing season only (Kozlowski 1992: 141) and is mainly responsible for the dendrometer signal at this period, along with possible changes in diameter because of the turgor pressure increase in spring (Deslauriers, Rossi & Anfodillo 2007). In other words, if the new bark and phloem corresponds to a fraction f_{DBH} of the total annual increment in the diameter at breast height (DBH), then the time $t_{0,i=0}$ when the first xylem cells are created corresponds to the moment where the normalized DBH curve reaches f_{DBH}. At the end of the growing season, the last xylem cells are produced at $t_{0,i=N}$, that we assume to correspond to the time when the DBH increase has attained 99.9% of the total annual increment. Finally, in-between $t_{0,0}$ and $t_{0,N}$, the starting dates $t_{0,i}$ are supposed to be equally spaced in time for simplification, although a Gompertz-type equation might be more appropriate (Rossi, Deslauriers & Morin 2003).

The cellulose deposition times Δt_i are assumed to be proportional to the cellulose content m_i of the sub-ring

$$\Delta t_i = \Delta \bar{t} \times \frac{m_i}{\bar{m}}, \qquad (11)$$

where $\Delta \bar{t}$ is an average deposition time and $\bar{m}$ is the mean cellulose content for a given tree ring. This definition of Δt_i is in line with the common observation that cellulose deposition lasts significantly longer for latewood than for early wood, at least in coniferous species (Kagawa *et al.* 2005; Vaganov, Anchukaitis & Evans 2009). In practice, m_i and $\bar{m}$ are proportional to the weights of each slice (measured after cellulose extraction). Therefore, only $\Delta \bar{t}$ needs to be prescribed.

Model parameterization

The list of parameters of the single-substrate model is given in Table 1.

A turnover rate k_{pool} of 10 year^{-1} means that the pool size adjusts itself to be refilled 10 times per year. If the annual biomass gain per tree (excluding litterfall) is $S_{biomass} = 10$ kgC tree^{-1} year^{-1} (a typical value for fast-growing forest plantations) this leads to an average pool size of 1 kgC tree^{-1}. Barbaroux, Bréda & Dufrene (2003) report typical values of total carbohydrate reserves in mature trees (including starch) of approximately 1.5–3 kgC tree^{-1} for *Quercus petraea* and *Fagus sylvatica*, depending on the season. Soluble sugars alone represent approximately 20% of this value (Barbaroux *et al.* 2003), that is, approximately 0.3–0.6 kgC tree^{-1}. In the following, we will use a value of $k_{pool} = 8$ year^{-1} and will also perform a sensitivity analysis to this parameter within the range 4–16 year^{-1}.

Because the simulation starts in winter (i.e. on 1 January in the northern hemisphere), the initial pool size is expected to be significantly smaller than the average pool size. However, tests show that the initial pool size $C_{pool,0}$ is not so critical because the model adjusts the pool size rapidly (within a few weeks), according to the value of k_{pool}. Similarly, initial values for the carbon and oxygen isotope ratios

Table 1. List of parameters of the single-substrate model, along with typical parameter values and range used for sensitivity analysis

Parameter	Value	Min|Max	Description
Parameters needed to compute C_{pool}			
$C_{pool,0}$ (kgC tree^{-1})	0.2		Initial sugar pool size
k_{pool} (year^{-1})	8	4|16	Whole-tree growth rate
Parameters needed to compute $\mathfrak{R}_{pool}$ (^{13}C/^{12}C only)			
$\delta_{pool,0}$ (VPDB)	−26‰		Initial ^{13}C/^{12}C ratio of the pool
x (−)	0‰	−1‰|1‰	Isotopic fractionation during wood formation (lignification)
Parameters needed to compute $\mathfrak{R}_{pool}$ (^{18}O/^{16}O only)			
$\delta_{pool,0}$ (VSMOW)	28‰		Initial ^{18}O/^{16}O ratio of the pool
x (−)	0‰	−1‰|1‰	Isotopic fractionation during wood formation (lignification)
Parameters needed to compute $\mathfrak{R}_{cellulose,i}$ (^{18}O/^{16}O only)			
p_{ex} (−)	0.3	0.2|0.4	Proportion of exchangeable oxygen during cellulose synthesis from sucrose
ε_{wc} (−)	27‰	26‰|28‰	Fractionation factor of carbonyl oxygen exchange with water
Parameters needed to compute $\mathfrak{R}_{cellulose,i}$ (^{13}C/^{12}C and ^{18}O/^{16}O)			
f_{DBH} (%)	20	10|30	Fraction of DBH signal caused by new bark and phloem formation
$\Delta \bar{t}$ (weeks)	2	1|4	Average number of weeks for complete cellulose deposition

Isotope ratios of the pool are expressed in 'delta' notations ($\delta = \mathfrak{R}/\mathfrak{R}_{std} - 1$), where $\mathfrak{R}_{std}$ is the isotope ratio of an international standard (VPDB for ^{13}C/^{12}C and VSMOW for ^{18}O/^{16}O).
VPDB, Vienna Peedee belemnite; VSMOW, Vienna Standard Mean Ocean Water.

Table 2. List of parameters used to compute $\mathfrak{R}_{assimilates}$

Parameter	Value	Min|Max	Description
Parameters needed to compute $\mathfrak{R}_{assimilates}$ ($^{13}C/^{12}C$ only or mainly)			
g_i [mol(air) m^{-2} s^{-1}]	0.10	0.05|0.15	Leaf internal conductance
g_{night} [mol(air) m^{-2} s^{-1}]	0.010	0.005|0.015	Leaf night-time conductance
b (−)	29‰	27‰|31‰	Net enzymatic carbon fractionation during CO_2 fixation
e (−)	0‰	−2‰|+2‰	Carbon isotopic fractionation during wood respiration
Parameters needed to compute $\mathfrak{R}_{assimilates}$ ($^{18}O/^{16}O$ only)			
V_{lw} [mol(H$_2$O) m^{-2}]	15	10|20	Leaf mesophyll water volume
L_{eff} (mm)	15	1|30	Leaf mesophyll effective mixing length

of the pool are not too critical. In the following, we will use $C_{pool,0} = 0.2$ kgC tree^{-1}, $\delta_{pool,0} = -26$‰ (for $^{13}C/^{12}C$) and $\delta_{pool,0} = +28$‰ (for $^{16}O/^{18}O$).

As described earlier, there is a lack of understanding of the isotope fractionation during lignification, hence we will use a value of $x = 0$‰ for both isotopes and will perform a sensitivity analysis to this parameter within the range ±2‰.

Different values of p_{ex} and ε_{wc} have been reported in the literature (Barbour *et al.* 2004; Cernusak *et al.* 2005; Sternberg *et al.* 2006). Preliminary tests revealed that our data suggest $p_{ex} = 0.3$ and $\varepsilon_{wc} = +27$‰ (or alternatively $p_{ex} = 0.4$ and $\varepsilon_{wc} = +28$‰), which is close to the values reported for natural day/night growth conditions with sucrose as the primary carbon source for cellulose synthesis (Cernusak *et al.* 2005; Sternberg *et al.* 2006). However, some uncertainties remain regarding these two parameters (Sternberg *et al.* 2006), and because of this a sensitivity analysis will also be performed.

Bark and new phloem thickness is quite variable among species. For *P. pinaster*, anatomical observations have shown that bark rings grow very early in the season and represent alone up to 10–15% of the total annual DBH increment (unpublished data). In addition, $t_{0,0}$ is more related to cell wall thickening rather than cell expansion and these two processes can be delayed by several weeks (Rossi *et al.* 2003; Deslauriers *et al.* 2008). In the following, we will use $f_{DBH} = 20\%$ and will perform a sensitivity analysis within the range 10–30%.

The duration for completing cellulose deposition in a given tree-ring section is quite variable among species and during the growing season. Cell wall thickening lasts typically approximately 2–3 weeks (Vaganov *et al.* 2009). In the following, we will use an average duration $\overline{\Delta t}$ for cellulose deposition time of 2 weeks (which generates values of Δt_i between 1 and 3 weeks, see Eqn 11) and will perform a sensitivity analysis to this parameter with values between 1 and 4 weeks.

Additional parameters are needed to compute $\mathfrak{R}_{assimilates}$ (Appendix A), and these are listed in Table 2.

Leaf internal conductance g_i is used to compute the ^{13}C discrimination during photosynthesis (Eqn A3), whereas night-time leaf stomatal conductance g_{night} is needed to compute leaf water ^{18}O enrichment during transpiration (Eqn A12), and therefore the $^{18}O/^{16}O$ ratio of current assimilates (Eqn A7). Typical values for evergreen

coniferous species are $g_i = 0.1$ mol(air) m^{-2} s^{-1} (Warren 2008) and $g_{night} = 0.01$ mol(air) m^{-2} s^{-1} (Caird, Richards & Donovan 2007). We will use these default values but will also perform a sensitivity analysis to these parameters within the range indicated in Table 2.

The net fractionation b of the enzyme-catalysed fixation of CO_2 by both ribulose 1·5-bisphosphate carboxylase/oxygenase (Rubisco) and phosphoenolpyruvate carboxylase (PEPC) is expected to lie within the range 27–30‰ (Farquhar *et al.* 1989). However, in C_3 plants, PEPC activity is usually very low, so that b should be closer to the value for Rubisco only [e.g. +29‰, see Roeske & O'Leary (1984)].

In natural conditions, CO_2 respired by heterotrophic tissues of adult trees is usually ^{13}C-enriched compared with the putative organic carbon source for respiration (Brandes *et al.* 2006; Gessler *et al.* 2007; Maunoury *et al.* 2007), with noticeable variations during the course of a day (Kodama, Barnard & Salmon 2008). However, this enrichment trend in CO_2 emitted from heterotrophic organs is not general and could even become a depletion, especially in herbaceous species (Badeck *et al.* 2005; Klumpp *et al.* 2005; Bathellier *et al.* 2009; Gessler *et al.* 2009). This difference in the isotope composition between the organic source and the product of respiration can result from a number of reasons: (1) fragmentation of the substrate molecule with heterogeneous isotope distribution (Schmidt & Gleixner 1998; Tcherkez *et al.* 2004); (2) re-fixation of respired CO_2 by PEPC (Badeck *et al.* 2005; Klumpp *et al.* 2005; Gessler *et al.* 2007, 2009); and (3) variations in the relative contribution to respired CO_2 from the Krebs cycle, the pyruvate dehydrogenase and pentose phosphate pathways (Dieuaide-Noubhani *et al.* 1995; Bathellier *et al.* 2009). This may result in an apparent fractionation during respiration, but does not necessarily imply that the isotope ratio of the carbohydrate pool ($\mathfrak{R}_{pool}$) is altered by respiration. In this paper, we will test the simplifying assumption that different carbon isotopic effects during woody respiration balance each other at the whole-plant level. The fractionation factor e will then be set to zero, and we will only perform a sensitivity analysis to this parameter within the range indicated in Table 2.

To compute the isotope ratio of leaf water $\mathfrak{R}_{lw}$, we need also two leaf parameters, V_{lw} and L_{eff}, the water volume and effective mixing length in the leaf mesophyll, respectively (see Appendix A). Although water volume V_{lw} is

constrained by leaf anatomy, the effective mixing length L_{eff} is more variable and a wide range of values has been reported in the literature (Wang & Yakir 1995). A typical value for V_{lw} in coniferous species is 15 mol m^{-2} (Seibt *et al.* 2007), whereas L_{eff} can range between 4 and 166 mm (Wang, Yakir & Avishai 1998), with more probable values ca. 15 mm (Barbour & Farquhar 2003).

MATERIAL AND METHODS

Experimental site

The experimental site where the data used for testing the model was collected is located approximately 20 km from Bordeaux, France (44°43′N, 0°46′W, 62 m a.s.l.) in a nearly homogeneous maritime pine stand (*P. pinaster*) planted in 1970. The trees are distributed in parallel rows along an NE–SW axis with an inter-row distance of 4 m. In 1997 (period at which the tree rings we studied were being formed) the stand density was 520 trees per hectare, the mean tree height was approximately 18 m and the leaf area index was approximately 3, that is, the whole-sided leaf area was ca. 6 m^2 leaf area m^{-2} ground area (Chen & Black 1992).

Meteorological and eddy flux measurements

The experimental setup that provided the meteorological and heat and CO_2 eddy flux measurements used here was installed following the requirements of the European project EUROFLUX. In particular, air temperature and relative humidity were measured every half-hour using a 50Y temperature-humidity probe (Vaisala, Vantaa, Finland). Soil water content in the root zone (down to −0.8 m) was recorded at least biweekly, using neutron probes or trace domain reflectometers. Other details can be found in Berbigier, Bonnefond & Mellmann (2001) and Ogée & Brunet (2002).

Sap flow and dendrometry measurements

Twelve trees within the stand were equipped with band dendrometers during years 1997 and 1998. Among this cluster, several trees were also equipped with electronic sensors for high-resolution sap flow and diameter increment measurements (at 1.3 m along an East–West axis). Sap flow sensors are described in Granier & Loustau (1994) and diameter increment sensors (point dendrometers) are as in Loustau, Domec & Bosc (1998).

Wood micro-densitometry measurements

A group of 17 trees, including those equipped with sap flow sensors and point dendrometers, was selected for micro-densitometry measurements. One 5-mm-wide core for each tree was sampled at breast height from pith to bark on the eastern azimuth. Each core was cut in 2-mm-long pieces, soaked in pentane for 24 h to remove resins and then stored at 12% humidity before exposure to X-rays (Seiffert Isovolt

3003 X-ray generator, GE Sensing & Inspection Technologies, http://www.geinspectiontechonologies.com). The radial density profile was obtained by analysing the digitalized X-ray images (Windendro Software, Regent Instruments Inc., Quebec, Canada) with a 25.4 μm resolution. Ring limits were automatically determined using this software then manually cross-dated.

Wood cellulose isotope measurements

Two trees were selected for intra-annual isotope measurements in wood cellulose. The trees were cored at breast height on an East–West axis using an increment borer with a large internal diameter (12 mm) in order to get enough material in each sample for all the isotope analysis (assuming at least 2 replicates per isotope species). The cores were then shaved with a cutter in the transversal plane and the tree-ring, early and late wood widths were measured by optical methods (Windendro Software, Regent Instruments Inc.). A short piece from each core including the 1997 and 1998 rings was cut and mounted on a sledge microtome (Leica 1400, Leica Microsystems, Bensheim, Germany). Contiguous, 100-μm-thick slices were cut parallel to the limits between rings. Each slice was then milled into very fine particles ($\leq$0.1 mm) using an ultra-centrifugal crusher (Retsch MM 300, Haan, Germany) and placed in small Teflon bags. Cellulose was extracted from the whole-wood samples using the technique described by Leavitt & Danzer (1993), adapted to small samples. For $\delta^{13}C$ and $\delta^{18}O$ measurements, 0.7–0.12 mg and 0.1–0.3 mg, respectively, of cellulose from the same sample was transferred in tin ($\delta^{13}C$) or silver ($\delta^{18}O$) capsules with at least two replicates. Isotopic analyses were performed by continuous flow methods as in Danis *et al.* (2006). The reproducibility of measurements carried out on an internal standard was better than 0.3‰ for $\delta^{18}O$ and 0.1‰ for $\delta^{13}C$. Isotopic ratios are expressed in 'delta' notation, that is, relative to international standards [Vienna Peedee belemnite (VPDB) for $\delta^{13}C$ and Vienna Standard Mean Ocean Water (VSMOW) for $\delta^{18}O$].

Leaf and soil water isotope measurements

During a single 22 h period, from 4 September 1997 at 0500 h (UTC) to 5 September 1997 at 0300 h (UTC), tree xylem and needle water samples as well as ambient air vapour samples were collected every hour. Soil profiles were also drilled from 0 to 0.5 m below the surface at 0930 h and 1330 h on 4 September 1997. All samples were then sent for water isotope analysis. Details can be found in Ogée *et al.* (2004).

Rain water isotope measurements

The oxygen isotope ratio of rain water is taken from the International Atomic Energy Agency/ World Meteorological Organization (IAEA/WMO) Global Network of Isotopes in Precipitation (GNIP; accessible at: http://isohis.iaea.org). The closest station from this network is

Brest-Plouzané (48.36°N, 4.57°W, 80 m a.s.l.), where monthly oxygen isotope data were available for the period 1997–1998. This station is quite far apart from our site, but the degree of continentality is very similar. Furthermore, during the period 1999–2004, the mean seasonal variations in the oxygen isotope composition of precipitation in Brest are very comparable with the variations in Dax, a more recent station much closer to our site (not shown). This gave us confidence that the GNIP data from Brest could be used as a good surrogate for estimating the isotope composition in precipitation at our site.

RESULTS

Climatic conditions

Monthly rainfall, air temperature and VPD measured at Le Bray during years 1997–1998 are shown in Fig 2. Compared with the values on the 1986–2006 period, also shown on this figure, year 1997 is characterized by two dry periods in spring (April–May) and at the end of summer (September–October), with high air VPD, high temperatures and rainfall deficits. In contrast, year 1998 seems to be a more 'normal' year, at least compared with the 1986–2006 period, with noticeable rainfall deficit and high VPD only in August.

Soil water model

Cumulative values of total evapotranspiration E_{tot} are shown in the top panel of Fig. 3, along with cumulative values of canopy transpiration ϕ_T (deduced from sap flow data, see Appendix A). These values of E_{tot} combined with the modelled values of the soil water drainage (Eqn B2) lead to a good agreement between measured and predicted variations of soil water content W_{soil} during 1997–1998, as shown in the middle panel of Fig. 3. Soil water content

reached very low levels for both years at the end of the summer. This end-of-summer drought is quite typical of this site. In contrast, soil water levels in spring are quite different between the two years, with unusually low values in 1997, in agreement with the higher air VPD and smaller cumulative rainfall at this period, compared with the 1998 and the 1986–2006 averages (Fig. 2).

The isotope ratio of soil water, $\Re_{sw}$, was computed using Eqn B4 and measured monthly values of the isotope ratio in precipitation $\Re_{rain}$. The temporal variations of these isotope ratios during the period 1997–1998 (expressed relatively to the international standard VSMOW) are shown in the bottom panel of Fig. 3. $\Re_{sw}$ remains close to $\Re_{rain}$ but exhibits smaller month-to-month variations because the size of the soil water pool is usually much larger than the monthly precipitation input.

Leaf gas-exchange and leaf water model

Measurements of leaf water isotopic enrichment conducted in different needles on 4 September 1997 and expressed relative to stem water at breast height are shown in Fig. 4, along with model results using Eqn A12 and other gas-exchange and isotopic forcing variables.

Interestingly, the experimental $\Delta^{18}O_{lw}$ values exhibit a rather similar diurnal cycle, regardless of needle age or position in the canopy (Fig. 4d). We can notice, however, a 2–3‰ shift between needles at the top and the bottom of the canopy, and a tendency for current-year needles to have a slightly larger diurnal amplitude, compared with older needles. Figure 4d also shows that the modelled $\Delta^{18}O_{lw}$ values obtained using Eqn A12 reproduce reasonably well the observed diurnal amplitude and are quite sensitive to V_{lw}, at least during daytime. On the other hand the model is almost insensitive to L_{eff} (not shown).
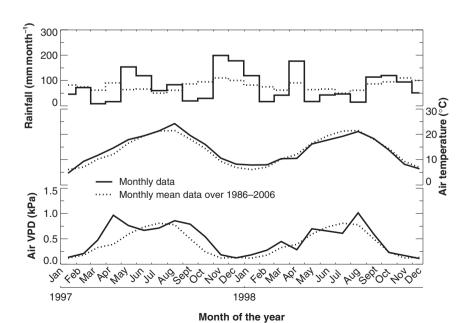

Figure 2. Monthly rainfall, air temperature and vapour pressure deficit at Le Bray in 1997 and 1998 (solid line) and during the period 1986–2006 (dotted line).
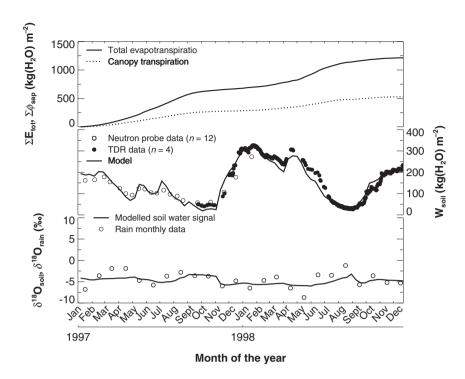
Figure 3. Water budget at Le Bray site during 1997–1998. Top panel: cumulative total evapotranspiration (eddy covariance data) and canopy transpiration (sap flow data). Middle panel: measured (with neutron probes or trace domain reflectometers) and modelled soil water content in the root zone (down to –0.8 m). Bottom panel: measured isotope ratio in precipitation (taken from Brest Global Network of Isotopes in Precipitation station) and modelled isotope ratio in soil water. TDR, Trace Domain Reflectometer.

The data shown in Fig. 4 was also used to test the assumption that atmospheric water vapour is close to isotopic equilibrium with soil water, $\Delta^{18}O_v = -\varepsilon^+$. This assumption is quite crude but seems to give reasonable estimates of the daily mean values, as shown in Fig. 4c. Furthermore, during this intensive field campaign, the predicted values of $\Delta^{18}O_{lw}$ did not change significantly when using the measured $\Delta^{18}O_v$ values rather than $-\varepsilon^+$ (not shown). On the contrary, Welp *et al.* (2008) recently found that using the isotopic equilibrium value for the water vapour $\delta^{18}O$, resulted in errors of ca. 2‰ on the assimilation-weighted leaf water isotopic enrichment $\Delta^{18}O_{lw}$ during the growing season. On a seasonal timescale, variations in $\delta^{18}O_v$ should be dominated by Rayleigh distillation processes associated with air-mass life cycles. A possible improvement could be then to calibrate a log-linear dependence between $\delta^{18}O_v$ and water vapour mixing ratio as described in Lee, Kim & Smith (2007). However, we do not have yet extensive measurements of water vapour to perform such a calibration at our site. In the following, and without more available data to check its validity, we will therefore assume that $\Delta^{18}O_v = -\varepsilon^+$ is a good approximation to model oxygen isotopic signals in tree ring cellulose.

Current assimilates and single-substrate pool model

Figure 5 shows 10 d minimum, maximum and flux-weighted mean values of the single-substrate pool size C_{pool} (computed using Eqn 3), the carbon and oxygen isotope ratios of current assimilates (using Eqns A2 and A7, respectively) and the carbon and oxygen isotope ratios of the pool.

The pool size C_{pool} is quite variable during the season with little difference between years and seasonal variations from approxiamtely 1 kgC tree^{-1} in winter to 3.5 kgC tree^{-1} in summer (Fig. 5a). Furthermore, we notice that C_{pool} never goes to zero, which is a direct consequence of Eqn 2 that links directly the demand of sink tissues to the pool size C_{pool}. The oxygen isotope composition of current assimilates (expressed in delta notations and noted $\delta^{18}O_{assimilates}$) is also quite variable during the season, with flux-weighted mean seasonal variations of ca. 15–20‰ (Fig. 5c). It also exhibits a large daily amplitude, approximately 15 ‰ throughout the season, and is strongly enriched in spring 1997 and more moderately at the end of the summer in both years. Similar conclusions can be drawn regarding the carbon isotope composition of current assimilates $\delta^{13}C_{assimilates}$ (Fig. 5e). This signal is also quite variable during the season, with a large daily amplitude, from approximately –40 to –12‰, caused by large daily fluctuations of the ratio C_c/C_a. The flux-weighted mean lies in-between these two extreme values and becomes enriched from May to September or even earlier in 1997 (dry spring), and depleted only in winter (from November–December to March–April). Finally, the daily variations of the carbon and oxygen isotope composition of the pool ($\delta^{13}C_{pool}$ and $\delta^{18}O_{pool}$, respectively) are strongly attenuated compared with $\delta^{13}C_{assimilates}$ or $\delta^{18}O_{assimilates}$, but their seasonal amplitude remains of the same size (Fig. 5b,d).

Wood growth periods, indicated by a shaded area in Fig. 5, have been deduced from the dendrometry data as explained in Fig. 6. In 1997, the growing period seems to start slightly earlier than in 1998, probably because of a warmer spring (Fig. 2). However, the DBH increase is much slower in 1997 than in 1998, possibly linked to low soil water
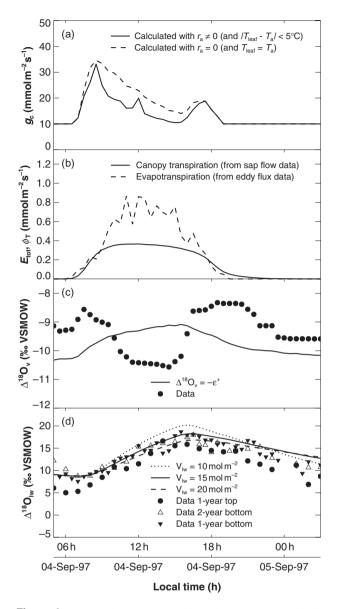
Figure 4. Modelled canopy stomatal conductance g_c, calculated with or without aerodynamical resistance (a), measured canopy transpiration ϕ_T and evapotranspiration E_{tot}, expressed on a whole-sided leaf area basis (b), measured and modelled oxygen isotope composition, expressed relative to soil water, of water vapour $\Delta^{18}O_v$ (c) and bulk leaf water $\Delta^{18}O_{lw}$ (d) at Le Bray site on 4 September 1997. Measured leaf values in current year needles at the top (1 year top) or the bottom (1 year bottom) of the canopy and previous-year needles at the bottom of the canopy (2 year bottom) are distinguished by different symbols. Modelled leaf water values are shown for the three different values of leaf mesophyll water volume V_{lw}. VSMOW, Vienna Standard Mean Ocean Water.

content in spring 1997 (Fig. 3). At the end of the growing season, the DBH increase rate slows down dramatically, which again seems to be linked with low soil water content (from July in 1998 and from August in 1997, see Fig. 3). However, wood growth (girth increment) does not seem to

stop until November, that is, when air temperature drops below ca. 13 °C (Fig. 2).

Cellulose isotopic ratios

Two trees have been selected for isotopic analysis. Ring width and mean wood density profiles during the period 1980–2007 are shown in Fig. 7 for these two individuals, as well as the average values for a larger group of 17 trees. Most individuals had very similar inter-annual variations of ring width and wood density in the 1980s and to a lesser extent in the 1990s. However, very different profiles can also be found in some individuals. Our first selected tree (tree n°1) falls in this category, whereas the other tree (tree n°2) is more typical of the whole stand. We might therefore expect quite different carbon and oxygen isotopic profiles in the wood cellulose of these two individuals.

These isotopic profiles (expressed in delta notations and noted $\delta^{13}C_{cellulose}$ and $\delta^{18}O_{cellulose}$ respectively) for the 1997–1998 rings are shown in Fig. 8. The temporal axis in this figure is expressed as the distance from the beginning of the 1997 ring, and therefore indicates the relative ring width. We can see that tree n°1 has about equal ring widths in 1997 and 1998, whereas tree n°2 has a larger ring in 1997 than in 1998, as confirmed by the dendrometry data shown in Fig. 7. Figure 8 also shows that the measured $\delta^{13}C_{cellulose}$ and $\delta^{18}O_{cellulose}$ signals in both trees exhibit a clear seasonal pattern for both isotope signals, but with a large variability between years and individuals. In 1997, the $\delta^{13}C$ signal becomes progressively enriched during the season with a distinct peak in the middle of the latewood for tree n°1 whereas, for the second tree, it remains steadily enriched during the entire 1997 season. That same year, the $\delta^{18}O_{cellulose}$ signals is very enriched in the early wood of tree n°2, which is not apparent in the other tree. Tree n°2 has a tendency to have a $\delta^{13}C_{cellulose}$ signal approximately 2‰ enriched compared with the other tree. It also exhibits weaker depletion in both $\delta^{13}C_{cellulose}$ and $\delta^{18}O_{cellulose}$ signals at the end of the 1997 growing season.

Figure 8 also shows the $\delta^{13}C_{cellulose}$ and $\delta^{18}O_{cellulose}$ signals predicted by our model. These modelled signals are different for the two individuals because the integration times Δt_i are different as they rely upon cellulose content (Eqn 11). However, the overall profiles are quite similar and in line with the seasonal variations in the $\delta^{13}C_{pool}$ and $\delta^{18}O_{pool}$ signals shown in Fig. 5. In particular, the model predicts a strong $\delta^{18}O_{cellulose}$ enrichment at the beginning of 1997 but not in 1998, in very good agreement with the measured values in tree n°2. Overall, the model matches reasonably well the measured profiles for both trees, especially in the 1997, although the model cannot compensate for the shift of ca. 2‰ in $\delta^{13}C$ observed between the two trees. In 1998, it seems that the model signal is delayed compared with the measurements, with quite depleted $\delta^{13}C_{cellulose}$ and $\delta^{18}O_{cellulose}$ values at the beginning of the early wood.
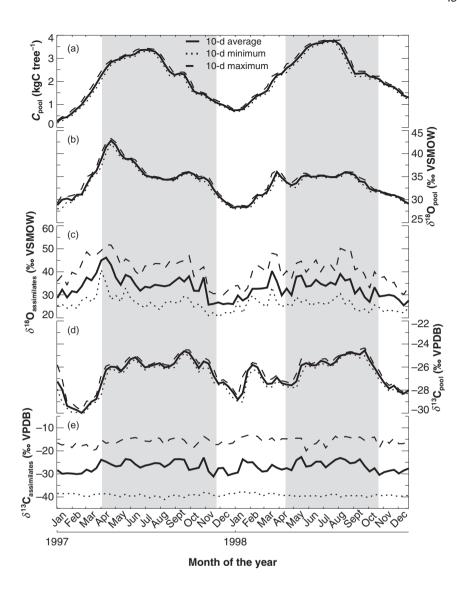
Figure 5. Results from the pool model using default parameter values from Tables 1 and 2. Modelled 10 d average values of sugar pool size C_{pool} (a), carbon and oxygen isotope ratios of the sugar pool $\delta^{13}C_{pool}$ (d) and $\delta^{18}O_{pool}$ (b) and current assimilates $\delta^{13}C_{assimilates}$ (e) and $\delta^{18}O_{assimilates}$ (c). The grey zones indicate the periods [$t_{0,0}$, $t_{0,N}$] during which wood cellulose is supposed to be formed (normalized diameter at breast height increment between 20% and 99.9% of total annual increment, see Fig. 6). VPDB, Vienna Peedee belemnite; VSMOW, Vienna Standard Mean Ocean Water.

Sensitivity analysis

Figure 9 shows how the mean modelled latewood isotopic signals ($\delta^{13}C_{LW}$ and $\delta^{18}O_{LW}$) is affected by each model parameter within the range indicated in Tables 1 and 2. These mean latewood isotopic signals are mostly influenced by the associated fractionation factors (e, b and x for $\delta^{13}C_{LW}$, ε_{wc}, p_{ex} and x for $\delta^{18}O_{LW}$), as well as the gas-exchange parameters g_{night} and g_i ($\delta^{13}C_{LW}$ only). The sensitivity of $\delta^{13}C_{LW}$ to g_{night} occurs because g_{night} is also used in the model as the minimum value for g_c. During latewood formation, drought tends to reduce g_c and brings it closer to g_{night} even during the daylight hours (Fig. 4a). The leaf water parameters L_{eff} and V_{lw} do not have strong effects on the $\delta^{18}O$ signal. As expected, the single-substrate pool turnover rate k_{pool} and the mean deposition time Δt_{mean} do not have strong effects on the mean latewood signals (Fig. 9) but rather on the short-term (within-ring) variations (not shown). Furthermore, the dendrometry parameter f_{DBH} only affects the

early-wood isotopic signals, because it mostly changes the starting date $t_{0,0}$.

DISCUSSION

Is the big-leaf approach a good approximation for tree-ring studies?

In the present model, isotopic discrimination processes during photosynthesis are described by considering only one single (big) leaf in the canopy (Appendix A). However, differences in the leaf water isotope composition of 2–3‰ are found between needles (Fig. 4d), which seems to indicate, for the same evaporative demand, higher stomatal conductances for needles at the top of the canopy (Farquhar, Cernusak & Barnes 2007). Similar differences in $\Delta^{18}O_{lw}$ have been reported in other species. Allison, Gat & Leaney (1985) observed, in the summer but not in spring, significant differences of leaf water
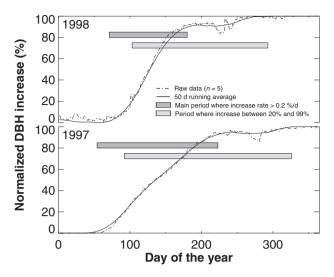
Figure 6. Normalized diameter at breast height (DBH) increase in 1997 and 1998 at Le Bray site, as deduced from point dendrometer measurements from three trees and two first-order branches. The 50 d running average is also shown, from which we calculated the main period when the normalized DBH increase rate is greater than 0.2% day^{-1} (dark grey bars) and the period when the normalized DBH increase was comprised between 25 and 99.9% of the annual total (light grey bars).

enrichment in *P. radiata* with position and needle age, whereas Shu *et al.* (2008) found that current-year needles were less enriched than previous-year needles in *P. resinosa* and *P. strobus*, but that the difference between the two cohorts of needles progressively weakened as young needles matured. This was attributed to differences in transpiration rate patterns along the needles (Shu *et al.* 2008). In this study, we use one single value for canopy transpiration and do not account for non-uniform patterns along needles. Given the encouraging model results shown in Fig. 8, we could conclude that neglecting these differences between needle age and position is a good approximation with regard to the isotopic signal in tree rings. However, it is not clear yet if a multilayer multi-leaf approach would not be more appropriate, because the present model is not strictly equivalent to a big-leaf canopy model. Canopy transpiration was measured (deduced from sap flow data) and canopy photosynthesis was computed by such a multilayer model (see Appendix A). In addition, using the multilayer canopy photosynthesis model CANISOTOPE, Baldocchi & Bowling (2003) showed that the relationship between canopy-scale water-use efficiency (the ratio of canopy CO_2 assimilation to canopy transpiration) and carbon isotope discrimination $\Delta^{13}C$ was positive because of the complex feedbacks among fluxes, leaf temperature and VPD, a finding that is counter to what is predicted for individual leaves. A proper comparison of multilayer and big-leaf approaches to model isotopic signals in wood cellulose is clearly needed.

Are Péclet effects in leaves important for tree-ring studies?

The big-leaf approach adopted here can partly explain why the leaf water isotope enrichment model remains quite insensitive to L_{eff}. Indeed, this lack of sensitivity to L_{eff} is caused by the small canopy transpiration rates, approximately 0.4 mmol m^{-2} s^{-1} at midday (Fig. 4b), caused by a strong stomatal control (Fig. 4a), but also because it represents an average (big leaf) value within the canopy. For higher individual transpiration rates approximately 3 mmol m^{-2} s^{-1}, we would obtain variations of the same order of magnitude as for V_{lw}, as shown by Cuntz *et al.* (2007) on individual sunlit *Lupinus angustifolius* leaves. During the growing season, canopy transpiration usually operates at higher rates than those shown in Fig. 4b because the soil water deficit is less pronounced (Fig. 3). However, even with values for ϕ_T approximately 1 mmol m^{-2} s^{-1}, Eqn A12 would remain quite insensitive to L_{eff}, as demonstrated by the lack of sensitivity of modelled $\delta^{18}O_{LW}$ values to this parameter (Fig. 9). These results question the usefulness of accounting for Péclet effects in this type of study and at this degree of model complexity.

What is leaf temperature?

On the other hand, the leaf water isotope enrichment model is quite sensitive to the way Eqn A9 is parameterized. Results shown in Fig. 4d have been obtained using a non-zero aerodynamical resistance for the computation of g_c (see Appendix A). Neglecting such a resistance would result in higher values of g_c (Fig. 4a) and approxiamtely 3‰ lower values of $\Delta^{18}O_{lw}$ at midday (not shown). The resulting diurnal cycle would then become too small compared with the measured one. Furthermore, the value for the fractionation factor during molecular diffusion used in Eqn A9 (28.5‰) is taken from Merlivat (1978), but a value of 32‰ has recently been proposed (Cappa *et al.* 2003) that would significantly increase the diurnal variations in $\Delta^{18}O_{lw}$. However, this new value was justified by evoking a surface cooling of several degrees at the liquid–air interface (the evaporative sites), compared with the bulk temperature of the liquid body. In our study T_s is a bulk canopy temperature deduced from the energy budget equation at the canopy scale, and tests revealed that a reduction of T_s by ca. 2 °C reduced ε^+ in a way that compensated nearly exactly the increase in ε_k from 28.5 to 32‰ (not shown). In other words, to reconcile these two studies, we could either use the value of 28.5‰ estimated by Merlivat (1978) without evoking surface cooling or that of 32‰ proposed by Cappa *et al.* (2003) after accounting for surface cooling. Because it would be quite arbitrary to apply a 2 °C reduction on T_s to compute $\Delta^{18}O_{lw}$, we decided to keep the value from Merlivat (1978) without evoking a surface cooling at the evaporative sites. However, a better understanding of the role of leaf temperature on the oxygen isotope composition of wood cellulose is clearly needed (Helliker & Richter 2008).
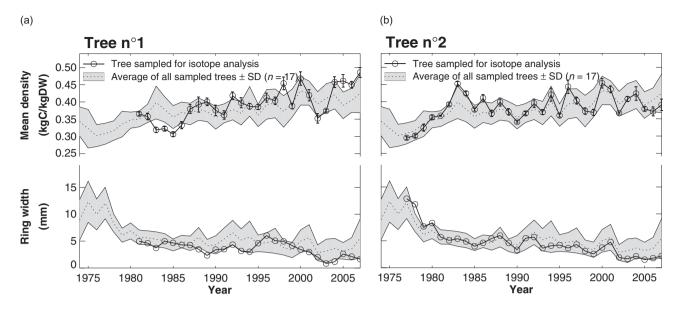
(a)

(b)

Figure 7. Mean wood ring density and width at Le Bray site, estimated from a set of 17 trees (one core per tree), and individual values for the two trees used for isotopic analysis: (a) tree n°1 and (b) tree n°2. Data missing before 1981 are caused by the damage on the tree core (all trees were planted in 1971). SD, standard deviation.

What dendrometers tell us about xylogenesis?

The amplitude of the seasonal changes in C_{pool} shown in Fig. 5a is consistent with those reported in the literature. For example, Damesin & Lelarge (2003) and Barbaroux & Bréda (2002) report seasonal shifts in soluble sugar concentrations of sapwood by a factor 2–3 between peak summer and winter in *F. sylvatica* and *Q. petraea*. In *P. sylvestris*, Hoch, Richter & Korner (2003) report nearly no variations in the

soluble content of branch sapwood and a twofold seasonal change in total non-structural carbohydrates, mainly attributed to starch reserves. In addition, as already observed by Klein *et al.* (2005) and Skomarkova *et al.* (2006), mean $\delta^{13}C_{assimilates}$ variations during the season (10‰) are much larger than $\delta^{13}C_{cellulose}$ (4‰ in our case, see Fig. 8). These variations are not caused by variations in the carbon isotope composition of air CO_2 that do not exceed 1‰ in our case (not shown). Furthermore, the strong enrichment of
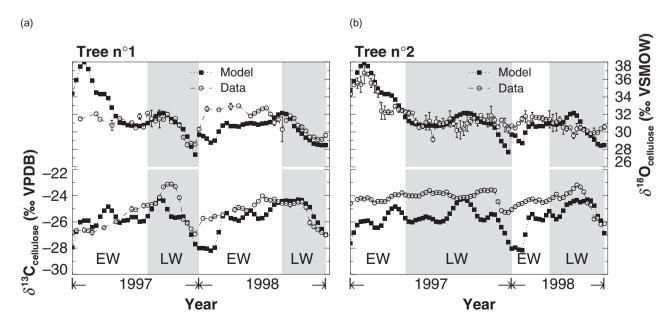
(a)

(b)

Figure 8. Cellulose data and model, obtained with default parameter values shown in Tables 1 and 2 for (a) tree n°1 and (b) tree n°2. Error bars on data are standard deviations of two to four replicates. EW, Early Wood; LW, Late Wood; VPDB, Vienna Peedee belemnite; VSMOW, Vienna Standard Mean Ocean Water.
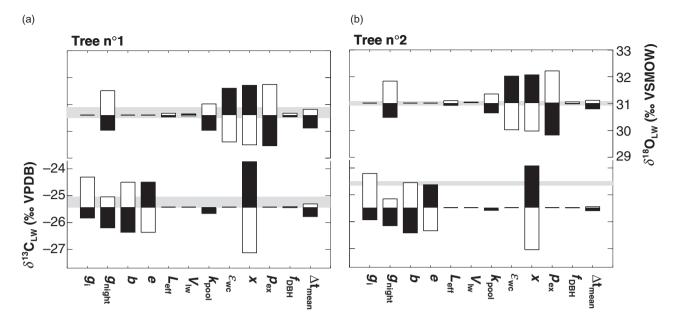
Figure 9. Mean changes in modelled isotopic signals in latewood cellulose across the range of a given parameter (all other parameters remaining to their default value) for (a) tree n°1 and (b) tree n°2. Parameter ranges and default values are given in Tables 1 and 2. Black boxes indicate an increase in the parameter with respect to the default value. Observed mean (±standard deviation) latewood cellulose signals are also indicated by a light grey zone. VPDB, Vienna Peedee belemnite; VSMOW, Vienna Standard Mean Ocean Water.

$\delta^{18}O_{assimilates}$ in spring 1997 and more moderately at the end of the summer in both years (Fig. 5c) is not caused by variations in the isotope composition of soil water (Fig. 3) but rather high levels of evaporative demand (Fig. 2).

Given the amplitude of variations of $\delta^{13}C_{assimilates}$ and $\delta^{18}O_{assimilates}$ during the growing season, it is clear that other damping effects are needed to link the signals to those recorded in wood cellulose (Fig. 8). The present model can do that, by means of a large and well-mixed pool (step 1) and long integration times Δt_i (step 2). The first step is illustrated in Fig. 5b and Fig. 5d, where we can see that the daily and seasonal variations of the carbon and oxygen isotope composition of the pool ($\delta^{13}C_{pool}$ and $\delta^{18}O_{pool}$, respectively) are strongly attenuated compared with $\delta^{13}C_{assimilates}$ or $\delta^{18}O_{assimilates}$. The second step is even simpler to anticipate, as it only consists in temporally averaging the pool signals during the times Δt_i (Eqn 8). These modelled pool signals, during the period $[t_{0,0}; t_{0,N}]$ indicated by a grey zone in Fig. 5, are therefore very similar but only more variable than the modelled cellulose signals shown in Fig. 8. For example, because wood growth stops around November, the very depleted values of $\delta^{13}C_{pool}$ and $\delta^{18}O_{pool}$ in winter will not be captured by the modelled cellulose signals. On the other hand, the strong enrichment of $\delta^{18}O_{pool}$ in early spring 1997 will be fully incorporated in the corresponding $\delta^{18}O_{cellulose}$ values, and in excellent agreement with the measurements (Fig. 8).

Studying the pool isotopic signals during the period $[t_{0,0}; t_{0,N}]$ also tells us why the model predicts depleted $\delta^{13}C_{cellulose}$ and $\delta^{18}O_{cellulose}$ values at the beginning of 1998 that are not recorded in the data. This is because, at the time when the dendrometry signal seems to indicate that

wood formation starts (mid-April in 1998), the pool values are still depleted, until the middle of May (Fig. 5). If we move the starting date $t_{0,0}$ (i.e. the beginning of the grey shaded area in Fig. 5) from mid-April to mid-May in 1998, the pool signals shown in Fig. 5 would remain unaffected but the $\delta^{13}C_{cellulose}$ and $\delta^{18}O_{cellulose}$ signals would no longer be depleted at the beginning of the early wood, and in much better agreement with the measurements (Fig. 10).

These results clearly demonstrate the need for a deeper understanding of what the dendrometry signal tells us about xylogenesis. Indeed, cell wall thickening can occur several weeks after cell enlargement, especially at the beginning of the growing season as observed in *P. cembra* and *P. leucodermis* growing in Italy (Rossi *et al.* 2003; Deslauriers *et al.* 2008). Thence, although girth increment is observed as soon as March in 1998, it could be that most of the cellulose synthesis (cell wall thickening) occurs later in the season. Interestingly, mid-May in 1998 corresponds to the time where soil water content in the root zone drops below ca. 120 mm (Fig. 3) and mean air temperature reaches 13 °C (Fig. 2). In 1997, this happens earlier in the season, at the end of March, and coincides with the $t_{0,0}$ value predicted by the dendrometry signal (Fig. 6). Maybe these thresholds on temperature and soil moisture are important signals for cellulose synthesis, and especially cell wall thickening. In spring, wood growth is unlikely limited by soil moisture, but temperature thresholds are commonly observed, especially in cold environment (Rossi *et al.* 2007; Deslauriers *et al.* 2008). Unfortunately the studies that explore the link between climate signals and xylogenesis are very time-consuming
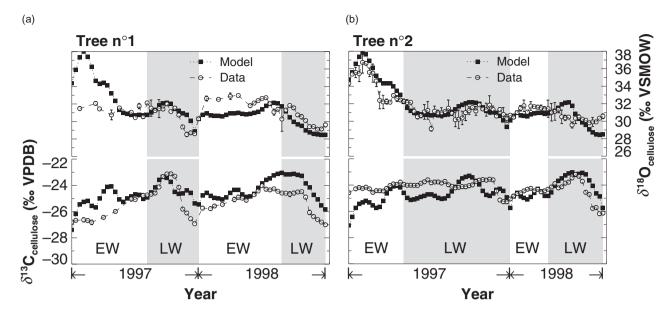
Figure 10. Cellulose data and model, obtained with default parameter values shown in Tables 1 and 2 and changes in $t_{0,0}$, $t_{0,N}$ and x (see related discussion) for (a) tree n°1 and (b) tree n°2. Error bars on data are standard deviations of two to four replicates. EW, Early Wood; LW, Late Wood; VPDB, Vienna Peedee belemnite; VSMOW, Vienna Standard Mean Ocean Water.

and cannot be performed on past climate because they require continuous histological measurements during the growing season (Rossi *et al.* 2003; Deslauriers *et al.* 2008). An interesting application of the current model could be to determine the best date $t_{0,0}$ required to fit the seasonal isotopic signals in cellulose, and therefore bring light on the link between $t_{0,0}$ (or the beginning of cell wall thickening t_{wt}) and climate variables during long time series.

Is the single-substrate hypothesis a good approximation?

Based on the sensitivity analysis shown in Fig. 9 and the discussion earlier, we could easily improve the model–data comparison by: (1) adjusting $t_{0,0}$ in 1998 (from mid-April to mid-May); (2) setting $t_{0,N}$ to 315 in 1997 (instead of 326 as deduced from the dendrometry signal); and (3) setting $x = +1‰$ for carbon isotopes only (in Fig. 9, the fractionation factor x influences both carbon and oxygen signals but, in theory, such a fractionation could occur only for the carbon isotopes). The agreement between data and model is very satisfactory (Fig. 10), although it could be improved even more knowing that dates $t_{0,i}$ should not necessarily be the same for all trees and should also not be spread uniformly within the interval [$t_{0,0}$, $t_{0,N}$] but rather follow a Gompertz-type distribution (Rossi *et al.* 2003). This demonstrates that the single-substrate hypothesis is a good approximation for *P. pinaster*, at least with the environmental conditions covered by this study. This result is in line with the preliminary study of Walcroft *et al.* (1997), but in conflict with the conclusions of other studies on other evergreen species (Hemming *et al.* 2001; Kagawa

et al. 2006). In fact, the current model seems to have almost too many degrees of freedom, as similar results as in Fig. 10 could be obtained without changing x but setting $b = 27‰$ or $e = +1.5‰$ instead (not shown). A more extensive dataset is needed to disentangle the effects of the fractionation factors x, e and b and demonstrate the need (or the lack of need) for a second pool of carbohydrates to interpret the intra-annual signals in the wood cellulose.

REFERENCES

Allison G.B., Gat J.R. & Leaney F.W.J. (1985) The relationship between deuterium and oxygen-18 values in leaf water. *Chemical Geology* **58,** 145–156.
Badeck F.-W., Tcherkez G., Nogués S., Piel C. & Ghashghaie J.

(2005) Post-photosynthetic fractionation of stable carbon isotopes between plant organs – a widespread phenomenon. *Rapid Communications in Mass Spectrometry* **19,** 1381–1391.

Baldocchi D.D. & Bowling D.R. (2003) Modelling the discrimination of $^{13}CO_2$ above and within a temperate broad-leaved forest canopy on hourly to seasonal time scales. *Plant, Cell & Environment* **26,** 231–244.

Barbaroux C. & Bréda N. (2002) Contrasting distribution and seasonal dynamics of carbohydrate reserves in stem wood of adult ring-porous sessile oak and diffuse-porous beech trees. *Tree Physiology* **22,** 1201–1210.

Barbaroux C., Bréda N. & Dufrene E. (2003) Distribution of above-ground and below-ground carbohydrate reserves in adult trees of two contrasting broad-leaved species (*Quercus petraea* and *Fagus sylvatica*). *New Phytologist* **157,** 605–615.

Barbour M.M. & Farquhar G.D. (2000) Relative humidity- and ABA-induced variation in carbon and oxygen isotope ratios of cotton leaves. *Plant, Cell & Environment* **23,** 473–485.

Barbour M.M. & Farquhar G.D. (2003) Do pathways of water movement and leaf anatomical dimensions allow development of gradients in $H_2^{18}O$ between veins and the sites of evaporation within the leaves? *Plant, Cell & Environment* **27,** 1–15.

Barbour M.M., Schurr U., Henry B.K., Wong S.C. & Farquhar G.D. (2000) Variations in the oxygen isotope ratio of phloem sap sucrose from castor bean. Evidence in support of the Péclet effect. *Plant Physiology* **123,** 671–679.

Barbour M.M., Andrews T.J. & Farquhar G.D. (2001) Correlations between oxygen isotope ratios of wood constituents of *Quercus* and *Pinus* samples from around the world. *Australian Journal of Plant Physiology* **28,** 335–348.

Barbour M.M., Walcroft A.S. & Farquhar G.D. (2002) Seasonal variation in $\delta^{13}C$ and $\delta^{18}O$ of cellulose from growth rings of *Pinus radiata*. *Plant, Cell & Environment* **25,** 1483–1499.

Barbour M.M., Roden J.S., Farquhar G.D. & Ehleringer J.R. (2004) Expressing leaf water and cellulose oxygen isotope ratios as enrichment above source water reveals evidence of a Péclet effect. *Oecologia* **138,** 426–435.

Barbour M.M., Hunt J.E., Dungan R.J., Turnbull M.H., Brailsford G.W., Farquhar G.D. & Whitehead D. (2005) Variation in the degree of coupling between $\delta^{13}C$ of phloem sap and ecosystem respiration in two mature *Nothofagus* forests. *New Phytologist* **166,** 497–512.

Bathellier C., Tcherkez G., Bligny R., Gout E., Cornic G. & Ghashghaie J. (2009) Metabolic origin of the $\delta^{13}C$ of respired CO_2 in roots of *Phaseolus vulgaris*. *New Phytologist* **181,** 387–399.

Berbigier P., Bonnefond J.-M. & Mellmann P. (2001) CO_2 and water vapour fluxes for 2 years above Euroflux forest site. *Agricultural and Forest Meteorology* **108,** 183–197.

Bernacchi C.J., Singsaas E.L., Pimentel C., Portis A.R. & Long S.P. (2001) Improved temperature response functions for models of Rubisco-limited photosynthesis. *Plant, Cell & Environment* **24,** 253–259.

Brandes E., Kodama N., Whittaker K., Weston C., Rennenberg H., Keitel C., Adams M.A. & Gessler A. (2006) Short-term variation in the isotopic composition of organic matter allocated from the leaves to the stem of *Pinus sylvestris*: effects of photosynthetic and postphotosynthetic carbon isotope fractionation. *Global Change Biology* **12,** 1922–1939.

Caird M.A., Richards J.H. & Donovan L.A. (2007) Nighttime stomatal conductance and transpiration in C3 and C4 plants. *Plant Physiology* **143,** 4–10.

Cappa C.D., Hendricks M.B., DePaolo D.J. & Cohen R.C. (2003) Isotopic fractionation of water during evaporation. *Journal of Geophysical Research* **108,** 4525. doi: 4510.1029/2003JD003597

Cernusak L.A., Pate J.S. & Farquhar G.D. (2002) Diurnal variation in the stable isotope composition of water and dry matter in fruiting *Lupinus angustifolius* under field conditions. *Plant, Cell & Environment* **25,** 893–907.

Cernusak L.A., Wong S.-C. & Farquhar G.D. (2003) Oxygen isotope composition of phloem sap in relation to leaf water in *Ricinus communis*. *Functional Plant Biology* **30,** 1059–1070.

Cernusak L.A., Farquhar G.D. & Pate J.S. (2005) Environmental and physiological controls over carbon and oxygen isotope composition of Tasmanian blue gum, *Eucalyptus globulus*. *Tree Physiology* **25,** 129–146.

Chen J.M. & Black T.A. (1992) Defining leaf area index for non-flat leaves. *Plant, Cell & Environment* **15,** 421–429.

Cuntz M., Ogée J., Farquhar G.D., Peylin P. & Cernusak L.A. (2007) Modelling advection and diffusion of water isotopologues in leaves. *Plant, Cell & Environment* **30,** 892–909.

Damesin C. & Lelarge C. (2003) Carbon isotope composition of current-year shoots from *Fagus sylvatica* in relation to growth, respiration and use of reserves. *Plant, Cell & Environment* **26,** 207–219.

Danis P.A., Masson-Delmotte V., Stievenard M., Guillemin M.T., Daux V., Naveau P. & von Grafenstein U. (2006) Reconstruction of past precipitation $\delta^{18}O$ using tree-ring cellulose $\delta^{18}O$ and $\delta^{13}C$: a calibration study near Lac d'Annecy, France. *Earth and Planetary Science Letters* **243,** 439–448.

Deslauriers A., Rossi S. & Anfodillo T. (2007) Dendrometer and intra-annual tree growth: what kind of information can be inferred? *Dendrochronologia* **25,** 113–124.

Deslauriers A., Rossi S., Anfodillo T. & Saracino A. (2008) Cambial phenology, wood formation and temperature thresholds in two contrasting years at high altitude in southern Italy. *Tree Physiology* **28,** 863–871.

Dewar R.C., Medlyn B.E. & McMurtrie R.E. (1998) A mechanistic analysis of light and carbon use efficiencies. *Plant, Cell & Environment* **21,** 573–588.

Dieuaide-Noubhani M., Raffard G., Canioni P., Pradet A. & Raymond P. (1995) Quantification of compartmented metabolic fluxes in maize root tips using isotope distribution from C-13 or C-14-labeled glucose. *Journal of Biological Chemistry* **270,** 13147–13159.

Dongmann G., Nürnberg H.W., Förstel H. & Wagener K. (1974) On the enrichment of $H_2^{18}O$ in the leaves of transpiring plants. *Radiation and Environmental Biophysics* **11,** 41–52.

Farquhar G.D. & Cernusak L.A. (2005) On the isotopic composition of leaf water in the non-steady state. *Functional Plant Biology* **32,** 293–303.

Farquhar G.D. & Lloyd J. (1993) Carbon and oxygen isotope effects in the exchange of carbon dioxide between terrestrial plants and the atmosphere. In *Stable Isotopes and Plant Carbon–Water Relations* (eds J.R. Ehleringer, A.E. Hall & G.D. Farquhar), pp. 47–70. Academic Press, San Diego, CA, USA.

Farquhar G.D. & Richards R.A. (1984) Isotopic composition of plant carbon correlates with water-use efficiency of wheat genotypes. *Australian Journal of Plant Physiology* **11,** 539–552.

Farquhar G.D., O'Leary M.H. & Berry J. (1982) On the relatioship between carbon isotope discrimination and the intercellular carbon dioxide concentrations in leaves. *Australian Journal of Plant Physiology* **9,** 121–137.

Farquhar G.D., Hubick K.T., Condon A.G. & Richards R.A. (1989) Carbon isotope fractionation and plant water-use efficiency. In *Stable Isotopes in Ecological Research* (eds P.W. Rundel, J.R. Ehleringer & K.A. Nagy), pp. 21–40. Springer-Verlag, New-York, NY, USA.

Farquhar G.D., Barbour M.M. & Henry B.K. (1998) Interpretation of oxygen isotope composition of leaf material. In *Stable*

Isotopes: Integration of Biological, Ecological and Geochemical Processes (ed. H. Griffiths), pp. 27–62. BIOS Scientfc Publishers Ltd., Oxford, UK.

Farquhar G.D., Cernusak L.A. & Barnes B. (2007) Heavy Water Fractionation during Transpiration. *Plant Physiol* **143,** 11–18.

Fritts H.C., Shashkin A.V. & Downes G.M. (1999) A simulation model of conifer ring growth and cell structure. In *Tree-ring Analysis: Biological, Methodological and Environmental Aspects* (eds R. Wimmer & R.E. Vetter), pp. 3–32. CAB International, Wallingford, UK.

Gessler A., Rennenberg H. & Keitel C. (2004) Stable isotope composition of organic compounds transported in the phloem of European beech – evaluation of different methods of phloem sap collection and assessment of gradients in carbon isotope composition during leaf-to-stem transport. *Plant Biology* **6,** 721–729.

Gessler A., Keitel C., Kodama N., Weston C., Winters A.J., Keith H., Grice K., Leuning R. & Farquhar G.D. (2007) $\delta^{13}C$ of organic matter transported from the leaves to the roots in *Eucalyptus delegatensis*: short-term variations and relation to respired CO_2. *Functional Plant Biology* **34,** 692–706.

Gessler A., Tcherkez G., Karyanto O., Keitel C., Ferrio J.P., Ghashghaie J., Kreuzwieser J. & Farquhar G.D. (2009) On the metabolic origin of the carbon isotope composition of CO_2 evolved from darkened light-acclimated leaves in *Ricinus communis*. *New Phytologist* **181,** 374–386.

Granier A. & Loustau D. (1994) Measuring and modelling the transpiration of a maritime pine canopy from sap-flow data. *Agricultural and Forest Meteorology* **71,** 61–81.

Gray J. & Thompson P. (1976) Climatic information from $^{18}O/^{16}O$ ratios of cellulose in tree rings. *Nature* **262,** 481–482.

Gray J. & Thompson P. (1977) Climatic information from $^{18}O/^{16}O$ analysis of cellulose, lignin and whole wood from tree rings. *Nature* **270,** 708–709.

Helle G. & Schleser G.H. (2004) Beyond CO_2-fixation by Rubisco – an interpretation of $^{13}C/^{12}C$ variations in tree rings from novel intra-seasonal studies on broad-leaf trees. *Plant, Cell & Environment* **27,** 367–380.

Helliker B.R. & Richter S.L. (2008) Subtropical to boreal convergence of tree-leaf temperatures. *Nature* **454,** 511–514.

Hemming D., Fritts H.C., Leavitt S.W., Wright W., Long A. & Shashkin A. (2001) Modelling tree-ring $\delta^{13}C$. *Dendrochronologia* **19,** 23–38.

Hoch G., Richter A. & Korner C. (2003) Non-structural carbon compounds in temperate forest trees. *Plant, Cell & Environment* **26,** 1067–1081.

Kagawa A., Sugimoto A., Yamashita K. & Abe H. (2005) Temporal photosynthetic carbon isotope signatures revealed in a tree ring through $^{13}CO_2$ pulse-labelling. *Plant, Cell & Environment* **28,** 906–915.

Kagawa A., Sugimoto A. & Maximov T.C. (2006) Seasonal course of translocation, storage and remobilization of ^{13}C pulse-labeled photoassimilate in naturally growing *Larix gmelinii* saplings. *New Phytologist* **171,** 793–804.

Klein T., Hemming D., Lin T., Grünzweig J.M., Maseyk K., Rotenberg E. & Yakir D. (2005) Association between tree-ring and needle $\delta^{13}C$ and leaf gas exchange in *Pinus halepensis* under semi-arid conditions. *Oecologia* **144,** 45–54.

Klumpp K., Schäufele R., Lötscher M., Lattanzi F.A., Feneis W. & Schnyder H. (2005) C-isotope composition of CO_2 respired by shoots and roots: fractionation during dark respiration? *Plant, Cell & Environment* **28,** 241–250.

Kodama N., Barnard R.L., Salmon Y., *et al.* (2008) Temporal dynamics of the carbon isotope composition in a *Pinus sylvestris* stand: from newly assimilated organic carbon to respired carbon dioxide. *Oecologia* **156,** 737–750.

Kozlowski T.T. (1992) Carbohydrates sources and sinks in woody plants. *The Botanical Review* **58,** 107–222.

Lanigan G.J., Betson N., Griffiths H. & Seibt U. (2008) Carbon Isotope Fractionation during Photorespiration and Carboxylation in *Senecio*. *Plant Physiology* **148,** 2013–2020.

Leavitt S.W. & Danzer S.R. (1993) Method for batch processing small wood samples to holocellulose for stable-carbon isotope analysis. *Analytical Chemistry* **65,** 87–89.

Lee X., Kim K. & Smith R. (2007) Temporal variations of the $^{18}O/^{16}O$ signal of the whole-canopy transpiration in a temperate forest. *Global Biogeochemical Cycles* **21,** GB3013. doi: 3010.1029/2006GB002871

Libby L.M., Pandolfi L.J., Payton P.H., Marshall J., Becker B. & Giertz-Sienbenlist V. (1976) Isotopic tree thermometers. *Nature* **261,** 284–288.

Loader N.J., Robertson I. & McCarroll D. (2003) Comparison of stable carbon isotope ratios in the whole wood, cellulose and lignin of oak tree-rings. *Palaeogeography, Palaeoclimatology, Palaeoecology* **196,** 395–407.

Loustau D., Domec J.-C. & Bosc A. (1998) Interpreting the variability of xylem sap flux density within the trunk of maritime pine (*Pinus pinaster* Aït.): application for calculating the water flux at the tree and stand levels. *Annales des Sciences Forestières* **55,** 29–46.

McCarroll D. & Loader N.J. (2004) Stable isotopes in tree rings. *Quaternary Science Reviews* **23,** 771–801.

Majoube M. (1971) Fractionnement en oxygène 18 et en deutérium entre l'eau et sa vapeur. *Journal de Chimie Physique* **68,** 1423–1436.

Maunoury F., Berveiller D., Lelarge C., Pontailler J.-Y., Vanbostal L. & Damesin C. (2007) Seasonal, daily and diurnal variations in the stable carbon isotope composition of carbon dioxide respired by tree trunks in a deciduous oak forest. *Oecologia* **151,** 268–279.

Merlivat L. (1978) Molecular diffusivities of $H_2^{16}O$, $HD^{16}O$ and $H_2^{18}O$ in gases. *Journal of Chemical Physics* **69,** 2864–2871.

Ogée J. & Brunet Y. (2002) A forest floor model for heat and moisture including a litter layer. *Journal of Hydrology* **255,** 212–233.

Ogée J., Brunet Y., Loustau D., Berbigier P. & Delzon S. (2003a) MuSICA, a CO_2, water and energy multilayer, multileaf pine forest model: evaluation from hourly to yearly time scales and sensitivity analysis. *Global Change Biology* **9,** 697–717.

Ogée J., Peylin P., Ciais P., Bariac T., Brunet Y., Berbigier P., Roche C., Richard P., Bardoux G. & Bonnefond J.-M. (2003b) Partioning net ecosystem exchange into net assimilation and respiration using $^{13}CO_2$ measurements: a cost-effective sampling strategy. *Global Biogeochemical Cycles* **17,** GB1070. doi: 1010.1029/2002GB001995

Ogée J., Peylin P., Cuntz M., Bariac T., Brunet Y. & Ciais P. (2004) Partitioning net ecosystem carbon exchange into net assimilation and respiration with canopy-scale isotopic measurements: an error propagation analysis with $^{13}CO_2$ and $CO^{18}O$ data. *Global Biogeochemical Cycles* **18,** GB2019. doi: 2010.1029/2003GB002166

Pate J. & Arthur D. (1998) $\delta^{13}C$ analysis of phloem sap carbon: novel means of evaluationg seasonal water stress and interpreting carbon isotope signatures of foliage and trunk wood of *Eucalyptus globules*. *Oecologia* **117,** 301–311.

Plomion C., Leprovost G. & Stokes A. (2001) Wood formation in trees. *Plant Physiol* **127,** 1513–1523.

Roden J.S., Lin G. & Ehleringer J.R. (2000) A mechanistic model for interpretation of hydrogen and oxygen isotope ratios in tree-ring cellulose. *Geochimica et Cosmochimica Acta* **64,** 21–35.

Roeske C.A. & O'Leary M.H. (1984) Carbon isotope effects on the enzyme-catalysed carboxylation of ribulose-1,5-biphosphate. *Biochemistry* **23,** 6275–6284.

Rossi S., Deslauriers A. & Morin H. (2003) Application of the Gompertz equation for the study of xylem cell development. *Dendrochronologia* **21,** 33–39.

Rossi S., Deslauriers A., Anfodillo T. & Carraro V. (2007) Evidence of threshold temperatures for xylogenesis in conifers at high altitudes. *Oecologia* **152,** 1–12.

Saurer M., Aellen K. & Siegwolf R. (1997) Correlating $\delta^{13}C$ and $\delta^{18}O$ in cellulose of trees. *Plant, Cell & Environment* **20,** 1543–1550.

Scartazza A., Mata C., Matteucci G., Yakir D., Moscatello S. & Brugnoli E. (2005) Comparisons of $\delta^{13}C$ of photosynthetic products and ecosystem respiratory CO_2 and their responses to seasonal climate variability. *Oecologia* **140,** 340–351.

Scheidegger Y., Saurer M., Bahn M. & Siegwolf R. (2000) Linking stable oxygen and carbon isotopes with stomatal conductance and photosynthetic capacity: a conceptual model. *Oecologia* **125,** 350–357.

Schiegl W.E. (1974) Climatic significance of deuterium abundance in growth rings of Picea. *Nature* **251,** 582–584.

Schmidt H.-L. & Gleixner G. (1998) Carbon isotope effects on key reactions in plant metabolism and 13C-patterns in natural compounds. In *Stable Isotopes: Integration of Biological, Ecological and Geochemical Processes* (ed. H. Griffiths), pp. 13–26. BIOS Scientifc Publishers Ltd., Oxford, UK.

Schultze B., Wirth C., Linke P., Brand W.A., Kuhlmann I., Horna V. & Schultze E.-D. (2004) Laser ablation-combustion-GC-IRMS – a new method for online analysis of intra-annual variation of $\delta^{13}C$ in tree rings. *Tree Physiology* **24,** 1193–1201.

Seibt U., Wingate L., Lloyd J. & Berry J.A. (2007) Nocturnal stomatal conductance effects on the $\delta^{18}O$ of foliage gas exchange observed in two forest ecosystems. *Tree Physiology* **27,** 585–595.

Shu Y., Feng X., Posmentier E.S., Faiia A.M., Ayres M.P., Conkey L.E. & Sonder L.J. (2008) Isotopic studies of leaf water. Part 2: between-age isotopic variations in pine needles. *Geochimica et Cosmochimica Acta* **72,** 5189–5200.

Skomarkova M.V., Vaganov E.A., Mund M., Knohl A., Linke P., Boerner A. & Schulze E.D. (2006) Inter-annual and seasonal variability of radial growth, wood density and carbon isotope ratios in tree rings of beech (*Fagus sylvatica*) growing in Germany and Italy. *Trees – Structure and Function* **20,** 571–586.

Sternberg L.D.S.L., De Niro M.J. & Savidge R.A. (1986) Oxygen isotope exchange between metabolites and water during biochemical reactions leading to cellulose synthesis. *Plant Physiology* **82,** 423–427.

Sternberg L., Pinzon M.C., Anderson W.T. & Jahren A.H. (2006) Variation in oxygen isotope fractionation during cellulose synthesis: intramolecular and biosynthetic effects. *Plant, Cell & Environment* **29,** 1881–1889.

Switsur R. & Waterhouse J. (1998) Stable isotopes in tree ring cellulose. In *Stable Isotopes: Integration of Biological, Ecological and Geochemical Processes* (ed. H. Griffiths), pp. 303–322. BIOS Scientific Publishers Ltd., Oxford, UK.

Tcherkez G. (2006) How large is the carbon isotope fractionation of the photorespiratory enzyme glycine decarboxylase? *Functional Plant Biology* **33,** 911–920.

Tcherkez G., Farquhar G.D., Badeck F.-W. & Ghashghaie J. (2004) Theoretical considerations about carbon isotope distribution in glucose of C_3 plants. *Functional Plant Biology* **31,** 857–877.

Vaganov E.A., Anchukaitis K.J. & Evans M.N. (2009) How well understood are the processes that create dendroclimatic records? In *Dendroclimatology: Progress and Prospects* (eds M.K. Hugues, T.W. Swetman & H. Diaz), Chapter 3. Springer-Verlag, New York, NY, USA.

Walcroft A.S., Silvester W.B., Whitehead D. & Kelliher F.M. (1997) Seasonal changes in stable carbon isotope ratios within annual rings of *Pinus radiata* reflect environmental regulation of growth processes. *Australian Journal of Plant Physiology* **24,** 57–68.

Wang X.F. & Yakir D. (1995) Temporal and spatial variations in the oxygen-18 content of leaf water in different plant species. *Plant, Cell & Environment* **18,** 1377–1385.

Wang X.-F., Yakir D. & Avishai M. (1998) Non-climatic variations in the oxygen isotopic compositions of plants. *Global Change Biology* **4,** 835–849.

Warren C.R. (2008) Stand aside stomata, another actor deserves centre stage: the forgotten role of the internal conductance to CO_2 transfer. *Journal of Experimental Botany* **59,** 1475–1487.

Welp L.R., Lee X., Kim K., Griffis T.J., Billmark K.A. & Baker J.M. (2008) $\delta^{18}O$ of water vapour, evapotranspiration and the sites of leaf water evaporation in a soybean canopy. *Plant, Cell & Environment* **31,** 1214–1228.

Whetten R. & Sederoff R. (1997) Lignin biosynthesis. *The Plant Cell* **7,** 1001–1017.

Wilson A.T. & Grinsted M.J. (1977) $^{12}C/^{13}C$ in cellulose and lignin as palaeothermometers. *Nature* **265,** 133–135.

Yakir D. (1998) Oxygen-18 of leaf water: a crossroad for plant-associated isotopic signals. In *Stable Isotopes: Integration of Biological, Ecological and Geochemical Processes* (ed. H. Griffiths), pp. 147–168. BIOS Scientific Publishers Ltd., Oxford, USA.

APPENDIX A: MODELLING THE ISOTOPIC DISCRIMINATION DURING PHOTOSYNTHESIS AND RESPIRATION

Discrimination against $^{13}CO_2$ during photosynthesis

Plants using C_3 metabolism discriminate against ^{13}C during net photosynthesis, resulting in plant tissue being depleted compared to atmospheric CO_2. At the leaf level this discrimination, noted $\Delta^{13}C$ (‰), may be expressed as (Farquhar, O'Leary & Berry 1982; Farquhar *et al.* 1989)

$$\Delta^{13}C \approx \bar{a} + (b - \bar{a})\frac{C_c}{C_a} - f\frac{\Gamma^*}{C_a}, \tag{A1}$$

where $\bar{a}$ is the average kinetic fractionation factor associated with diffusion of CO_2 through the boundary-layer, stomata and leaf lamina, b is the net kinetic fractionation of the enzyme-catalysed fixation of CO_2 by both Rubisco and PEP carboxylase, f ($\approx 11‰$) is the fractionation during photorespiration (Tcherkez 2006; Lanigan *et al.* 2008), Γ^* (mol mol^{-1}) is the CO_2 compensation point in the absence of day respiration, which depends on leaf temperature (Bernacchi *et al.* 2001) and C_c and C_a (mol mol^{-1}) are the partial pressures of CO_2 at the carboxylation sites inside the leaf chloroplasts and in the atmosphere, respectively. Note that Eqn A1 neglects isotopic effects because of day respiration

but other fractionations, during wood respiration but also night-time foliage respiration, are accounted for and lumped together in one single factor e (see discussions on carbon and oxygen isotope signals of the sugar pool, and model parameterization). The fractionation factor $\bar{a}$ can be computed as a linear combination of the fractionation factors that occur during the different diffusional steps (see further discussion).

Equation A1 only applies to the very first products of photosynthesis. The $^{13}C/^{12}C$ isotope ratio of these current assimilates ($\mathfrak{R}_{assimilates}$) is then equal to the $^{13}C/^{12}C$ isotope ratio of atmospheric CO_2 ($\mathfrak{R}_a$) divided by $1 + \Delta^{13}C$

$$\mathfrak{R}_{assimilates} = \frac{\mathfrak{R}_a}{1 + \Delta^{13}C}. \tag{A2}$$

Because $\Delta^{13}C > 0$, this equation shows that current assimilates are depleted compared to atmospheric CO_2.

In this study we will assume that Eqn A1 can be applied at the tree or canopy scale. The kinetic fractionation factor $\bar{a}$ will then be computed as (Farquhar *et al.* 1989; Ogée *et al.* 2003b)

$$\bar{a} = \frac{2.9g_c + 4.4g_b + 1.8g_c g_b / g_i}{g_c + g_b + g_c g_b / g_i}, \tag{A3}$$

where g_c [mol(air) m^{-2} s^{-1}] is the canopy stomatal conductance for CO_2, g_b [mol(air) m^{-2} s^{-1}] is the canopy leaf boundary-layer conductance for CO_2 diffusion in air, g_i [mol(air) m^{-2} s^{-1}] is the canopy internal conductance to CO_2 diffusion through the leaf mesophyll.

Equation A3 was obtained by using the standard 'big-leaf' multiple resistance model. In this framework, C_c/C_a is given by

$$\frac{C_c}{C_a} = 1 - \frac{F_{leaf}}{M_C C_a}\left(\frac{1}{g_a} + \frac{1}{g_c} + \frac{1}{g_i}\right), \tag{A4}$$

where M_C (0.012 kg mol^{-1}) is the molar weight of carbon and $g_a = (g_b^{-1} + g_t^{-1})^{-1}$ is the aerodynamical conductance for CO_2 through leaf (g_b) and turbulent (g_t) boundary layers.

Eddy flux measurements were used to compute the aerodynamic conductance for CO_2 g_a [mol(air) m^{-2} s^{-1}], as described in Ogée *et al.* (2003b). Net leaf photosynthesis F_{leaf} could not be simply deduced from CO_2 eddy flux measurements because of the presence of an active understorey that contributes significantly to the net ecosystem carbon exchange. Instead, we used F_{leaf} estimates from the multi-layer model MuSICA that had already been carefully calibrated and validated at our site (Ogée *et al.* 2003a). The same model was used to compute wood respiration F_{wood} used in Eqn 3 in the main discussion.

Stomatal conductance to CO_2 g_c [mol(air) m^{-2} s^{-1}] was computed from sap flow data ϕ_{sap} [mol(H_2O) m^{-2} s^{-1}]. In order to account for water capacitance effects within the tree, tree transpiration ϕ_T was first computed assuming a lag of 1.5 h in advance compared to ϕ_{sap}, that is,

$\phi_T(t) = \phi_{sap}(t + 1.5\,h)$. This lag was chosen so that ϕ_T was in phase with the latent heat flux measured above the canopy by eddy covariance. Stomatal conductance was then computed according to

$$\frac{1}{1.6g_c} = \frac{w_i - w_a}{\phi_T} - \frac{1}{g_a'}, \tag{A5}$$

where w_i and w_a (mol mol^{-1}) are the partial pressures of water vapour inside the leaf and in the atmosphere, respectively, and g_a' [mol(air) m^{-2} s^{-1}] is the counterpart of g_a for water vapour and is computed as in Ogée *et al.* (2003b). The 1.6 factor arises from the conversion of conductances for CO_2 to conductances for water vapour. The partial pressure deficit $w_i - w_a$ is further computed using a first-order Taylor series

$$w_i - w_a \approx [w^*(T_a) - w_a] + \left.\frac{dw^*}{dT}\right|_{T_a} \cdot (T_s - T_a), \tag{A6}$$

where w^* (mol mol^{-1}) is the water vapour partial pressure at saturation and leaf temperature T_s (K). The difference $T_s - T_a$ is computed from sensible heat flux data and aerodynamic conductance [see Ogée *et al.* (2003b) for details]. Because sensible heat flux data contains contributions from all surfaces, including soil and understorey, this can create unrealistic values of leaf temperature ($T_s - T_a$ up to 10 °C) when we expect the needles to be relatively well-coupled to the atmosphere. We therefore limited the difference $|T_s - T_a|$ to stay smaller than 5 °C.

Oxygen isotope effects during photosynthesis

Photoassimilates exported from source leaves have been found to be in oxygen isotopic equilibrium with average leaf mesophyll water (Barbour *et al.* 2000; Cernusak, Wong & Farquhar 2003):

$$\mathfrak{R}_{assimilates} = \mathfrak{R}_{lw}\alpha_{wc}, \tag{A7}$$

where α_{wc} [≈1.027, Sternberg *et al.* (1986)] is the fractionation associated with isotopic exchange between carbonyl oxygen and water and $\mathfrak{R}_{lw}$ is the average isotope ratio of leaf mesophyll water. Water in the mesophyll gets enriched compared with source (soil) water because of leaf evaporation. At the sites of evaporation and in the steady state, this enrichment $\Delta^{18}O_{es,0}$ can be modelled as (Dongmann *et al.* 1974; Farquhar & Lloyd 1993)

$$\Delta^{18}O_{es,0} = \varepsilon^+ + \varepsilon_k + (\Delta^{18}O_v - \varepsilon_k)\frac{w_a}{w_i}, \tag{A8}$$

where ε^+ (‰) is the equilibrium fractionation during the phase change from liquid to vapour, ε_k (‰) is the kinetic fractionation factor caused by the diffusion of water vapour through stomata and leaf boundary layer and $\Delta^{18}O_v$ (‰) is the ^{18}O enrichment above source water of atmospheric vapour. The equilibrium fractionation factor, ε^+, is dependent on leaf temperature and is computed according to

Majoube (1971). In a similar manner as for $\bar{a}$, the kinetic fractionation factor ε_k is calculated from bulk canopy and boundary-layer conductances for water vapour (Farquhar *et al.* 1989; Farquhar & Lloyd 1993):

$$\varepsilon_k = \frac{28.5 g_b' + 18.9 \times 1.6 g_c}{g_b' + 1.6 g_c}. \tag{A9}$$

Average mesophyll water is less enriched than the sites of evaporation because of an advection-diffusion process. In the steady state, this effect may be modelled as (Farquhar & Lloyd 1993):

$$\Delta^{18}O_{lw,0} = \frac{\Delta^{18}O_{es,0}(1 - e^{-\wp})}{\wp}, \tag{A10}$$

where $\Delta^{18}O_{lw,0}$ is the average mesophyll water enrichment above source water and $\wp$ is the Péclet number that compares advection and back-diffusion fluxes in the leaf mesophyll:

$$\wp = \frac{\phi_T / S_{leaf}}{C_w D_{diff} / L_{eff}}, \tag{A11}$$

where S_{leaf} (m^2 m^{-2}) is whole-sided leaf area per ground area (required if ϕ_T is expressed on a ground area basis), $C_w = 55.5$ mol(H$_2$O) m^{-3} is the molar concentration of liquid water, L_{eff} (m) is the effective mixing length and D_{diff} (m^2 s^{-1}) is the tracer diffusion of H$_2^{18}$O in normal water. The latter is temperature-dependent and equals $2.25\ 10^{-9}$ m^2 s^{-1} at 25 °C (Cuntz *et al.* 2007).

Equation A10 is valid in the steady state only and is unlikely to give accurate predictions of average leaf water enrichment in the field, especially at night (Cernusak, Pate & Farquhar 2002). A non-steady-state model has then been developed, which shows good agreement with measurements (Farquhar & Cernusak 2005; Cuntz *et al.* 2007). The non-steady-state enrichment of average leaf water ($\Delta^{18}O_{lw}$) satisfies the differential equation (Farquhar & Cernusak 2005; Cuntz *et al.* 2007)

$$\frac{d(V_{lw} \cdot \Delta^{18}O_{lw})}{dt} = \frac{g_c w_i}{\alpha_k \alpha^+} \cdot \frac{\wp}{1 - e^{-\wp}} (\Delta^{18}O_{lw,0} - \Delta^{18}O_{lw}), \tag{A12}$$

where $\alpha_k = 1 + \varepsilon_k$, $\alpha^+ = 1 + \varepsilon^+$ and V_{lw} [mol(H$_2$O) m^{-2}] is the lamina mesophyll water content. The isotope ratio of average lamina mesophyll water is then computed as

$$\mathfrak{R}_{lw} = (1 + \Delta^{18}O_{lw})\mathfrak{R}_{sw}. \tag{A13}$$

In practice, we need to know the oxygen isotope composition of water vapour ($\Delta^{18}O_v$) to predict $\mathfrak{R}_{lw}$ (Eqn A8). During the growing season, we will assume that the isotopic content of water vapour in the air, $\mathfrak{R}_v = (1 + \Delta^{18}O_v)\mathfrak{R}_{sw}$, is in isotopic equilibrium with soil water, that is, $\mathfrak{R}_v = \mathfrak{R}_{sw}/\alpha^+$ (or alternatively $\Delta^{18}O_v = -\varepsilon^+$)

APPENDIX B: MODELLING THE ISOTOPE COMPOSITION OF SOIL WATER

The oxygen isotope ratio of soil water ($\mathfrak{R}_{sw}$) is needed to compute the isotope ratios of leaf water ($\mathfrak{R}_{lw}$, see Eqn A13) and wood cellulose (Eqn 10). For that the soil water content in the root zone [W_{soil}, kg(H$_2$O) m^{-2}] is first computed using half-hourly values of local precipitation [P, kg(H$_2$O) m^{-2} s^{-1}] and total evapotranspiration [E_{tot}, kg(H$_2$O) m^{-2} s^{-1}], as in Ogée & Brunet (2002):

$$\frac{dW_{soil}}{dt} = P - E_{tot} - D, \tag{B1}$$

where D [kg(H$_2$O) m^{-2} s^{-1}] is drainage below the root zone. Because the site is on a flat terrain, runoff is negligible. E_{tot} accounts for canopy and understorey transpiration as well as soil evaporation and is directly deduced from latent heat eddy-covariance flux data. Drainage is further computed as

$$D = k_{soil}(W_{soil} - W_{soil,min}), \tag{B2}$$

where k_{soil} (s^{-1}) and $W_{soil,min}$ [kg(H$_2$O) m^{-2}] are constant parameters [0.012 s^{-1} and 80 kg(H$_2$O) m^{-2} at our site, respectively, see Ogée & Brunet (2002)].

The budget of soil water isotopes in the root zone is then computed in a similar fashion:

$$\frac{d\mathfrak{R}_{sw}W_{soil}}{dt} = \mathfrak{R}_{rain}P - \mathfrak{R}_{sw}(E_{tot} - E_{soil}) - \mathfrak{R}_{evap}E_{soil} - \mathfrak{R}_{sw}D, \tag{B3}$$

where $\mathfrak{R}_{sw}$ is the ^{18}O/^{16}O isotopic ratio of bulk soil water, $\mathfrak{R}_{rain}$ is the ^{18}O/^{16}O isotopic ratio of rain and $\mathfrak{R}_{evap}$ is the ^{18}O/^{16}O isotopic signature of soil evaporation.

According to Ogée & Brunet (2002), evaporation from the forest floor is approximately 10% of the total evapotranspiration E_{tot}. However, soil evaporation *per se* is expected to be much lower because most of the evaporation comes usually from the litter layer (Ogée & Brunet 2002). In this study, we will assume that E_{soil} is zero. Equation B3 then is simplified to

$$\frac{d\mathfrak{R}_{sw}W_{soil}}{dt} = \mathfrak{R}_{rain}P - \mathfrak{R}_{sw}(E_{tot} + D). \tag{B4}$$